DOE/ER/60539-11

FINAL PROGRESS REPORT

Grant DE-FG02-87ER60539

U.S. Department of Energy Washington, D.C.

Project Title: The Oncogenic Action of Ionizing Radiation on Rat Skin

Institution: Department of Environmental Medicine,
New York University Medical Center
550 First Avenue
New York, NY 10016

Principal Investigator: Fredric J. Burns, Ph.D.

Co-investigator: Seymour J. Garte, Ph.D

Period Covered by the Report: May 1, 1990 through April 30, 1992

DISCLAIMER

Summary of Progress

This section includes descriptions of results from previous studies. These studies are based on the belief that a thorough understanding of radiation carcinogenesis in a single organ system is the most likely way to achieve a general understanding of the process. We have found that a useful model to analyze radiation carcinogenesis in rat skin is the modified dual action hypothesis. In this hypothesis 2 initial events resulting in heritable molecular changes are postulated as the starting point for several measurable endpoints of biological damage including cancer induction.

The multistage theory of carcinogenesis specifies that cells progress to cancer through a series of discrete, irreversible genetic alterations, but data on radiation-induced cancer incidence in rat skin suggests that an intermediate repairable alteration may occur. Data are presented on cancer induction in rat skin exposed to the following radiations: 1. an electron beam (LET=0.34 kev/μ), 2. a neon ion beam (LET=45 kev/μ) and 3. an argon ion beam (LET=125 kev/μ). The latter 2 beams were generated by the Bevalac at the Lawrence Berkeley Laboratory, Berkeley, CA. About 6.0 cm^2 of skin was irradiated per rat. The rats were observed every 6 weeks for at least 78 weeks and tumors were scored at first occurrence. Several histological types of cancer, including squamous and basal cell carcinomas, were induced. The total cancer yield was fitted by the quadratic equation, and the equation parameters were estimated by linear regression for each type of radiation. Analysis of the DNA from the electron-induced carcinomas indicated that K-*ras* and/or c-*myc* oncogenes were activated in all tumors tested. *In situ* hybridization indicated that the cancers contain subpopulations of cells with differing amounts of c-*myc* and H-*ras* amplification. The results are consistent with the idea that ionizing radiation produces stable, carcinogenically relevant lesions via 2 repairable events at low LET and via a non-repairable, linked event pathway at high LET; either pathway may advance the cell by 1 stage in the multistage model.

The proliferative response of rat epidermis following exposure to ionizing radiation was quantified. An injection of ^{14}C-thymidine in 27 day old, male rats labeled a cohort of S-

phase cells and defined time zero. The return of these cells to S-phase a second time was detected by a second label (^{3}H-thymidine) at various later times. At 18 hrs, when the ^{14}C-labeled cells were well into the G1-phase, the dorsal skin was either sham irradiated or irradiated with 10 Gy or 25 Gy of 10 KvP X-rays. Immediately after irradiation the skin surface was stripped with cellophane tape to stimulate proliferation in the basal cells. Skin biopsies were taken at approximately 12 hr intervals for 124 hrs and incubated in 10 μc/ml of ^{3}H-thymidine. The ^{3}H, ^{14}C and ^{3}H + ^{14}C labeling indices were determined by counting cells on the double emulsion autoradiographs under oil immersion light microscopy. The ^{14}C labeling index was constant and unaffected by the radiation. The proportion of all cells entering S-phase, i.e. the ^{3}H labeling index, averaged 3.5% at 18 hrs and increased after 44, 52 and 75 hrs to average levels of 11.8%, 5.3%, and 6.6% at 0 Gy, 10 Gy and 25 Gy respectively. The proportion of S-phase cells labeled with ^{14}C ("labeled S-phase") increased after 42 hrs and remained relatively constant thereafter at average values of 2.8%, 2.8% and 3.7% at 0 Gy, 10 Gy and 25 Gy, respectively. The proportion of ^{14}C-labeled cells that entered S-phase closely paralleled the proportion of all cells entering S-phase. The proportion was low at first then increased after 53 hrs to average levels of 10.0% at 0 Gy, 3.5% at 10 Gy and 4.0% at 25 Gy. These results are consistent with the proliferative stimulus acting to increase the rate of transfer of cells from a G_0 phase into pre-S-phase and S-phase, while the major effect of the radiation was to reduce the increased rate of transfer of all cells, including the ^{14}C-labeled cohort, from G_0-phase into S-phase.

The c-*myc* oncogene may play a role in controlling cell proliferation and in converting irradiated cells to cancer cells. C-*myc* amplification has been detected by Southern blotting in radiation-induced rat skin tumors, including squamous and basal cell carcinomas. *in situ* hybridization was utilized in the present experiment in order to examine the localization of c-*myc* amplification within the cancers. A biotinylated human c-*myc* third exon probe, visualized with an avidin-biotinylated alkaline phosphatase detection system was used. The incorporation of ^{3}H-thymidine into the DNA of rat skin cells showed that the proliferation rate of

epidermal cells reached a peak on the seventh day after exposure to ionizing radiation and then decreased. No c-*myc* oncogene amplification was detected in normal rat skin at very early times after exposure to ionizing radiation, which is consistent with the view that c-*myc* amplification is more involved in carcinogenesis than in normal cell proliferation. The results indicated that c-*myc* amplification as measured by *in situ* hybridization was correlated with previous Southern blot results, but within each cancer only some of the cells exhibited amplification. The c-*myc* positive cells were distributed randomly within the tumor and exhibited a more uniform nuclear structure in comparison to the more vacuolated c-*myc* negative cells. No c-*myc* signal was detected in unirradiated normal skin or in irradiated skin cells near the tumors. c-*myc* amplification appears to be cell or cell cycle specific within radiation-induced carcinomas.

The c-*myc* oncogene was previously shown to be amplified in large, later stage carcinomas of the rat skin induced by 0.8 MeV electrons. In a panel of over 70 tumors induced by high LET (45 Kev/μ) neon ions, c-*myc* amplification was rare, and in contrast to the low LET (0.3 Kev/μ) tumor data, showed no correlation with tumor size, growth period or time. Furthermore, the tumor tissue specificity seen with low LET tumors was not seen in the high LET panel. These results suggest that quite distinct molecular mechanisms operate even in late stages of tumorigenesis that depend on the LET of the inducing radiation. Furthermore, the results suggest that c-myc amplification observed in low LET induced tumors is not a general property of rat skin carcinomas, but is mechanistically linked to the inducing radiation, even though it is not detectable until many months after exposure.

Detailed Description of Progress

Progress has occurred in several areas corresponding to the specific aims of the proposal: 1) Progression and multiple events in radiation carcinogenesis of rat skin as a function of LET; 2) Cell cycle kinetics of irradiated rat epidermis as determined by double labeling and double emulsion autoradiography; 3) Oncogene activation detected by *in situ* hybridization in radiation-induced rat skin tumors; 4) Amplification of the c-*myc* oncogene in radiation-induced

rat skin tumors as a function of LET; and 5) Transformation of rat skin keratinocytes by ionizing radation in combination with c-Ki-*ras* and c-*myc* oncogenes.

1.0 *Progression and Multiple Events in Radiation Carcinogenesis of Rat Skin*

Exposure of rat skin to ionizing radiation elicits a variety of tumor types including, squamous carcinomas, basal cell carcinomas, clear cell carcinomas, sarcomas and miscellaneous other tumors. The variety of different types of cancers reflects the variety of cell types found in skin. Rat skin has been used extensively to study the dose-response and time-response characteristics of radiation-induced epithelial cancer and for investigating how early biological events associated with the absorption of the radiation cause a cell to embark on the pathway to cancer (1). A comparison of radiation-induced cancer incidence in animals relative to human epidemiological data is available for skin (2,3).

The multistage theory of carcinogenesis was originally invoked to explain the temporal pattern of cancer incidence data in human populations (4). Recent versions of this theory, especially the 2 stage version, have been postulated to explain aspects of experimental chemical carcinogenesis in animals, e.g., initiation and promotion in mouse skin, and more recently the occurrence of multiple oncogene activations in experimental tumors (5,6) (Figure 1). Each transition, two of which are illustrated, is considered to be a permanent genetic alteration that is transmitted to daughter cells and represents another step in the "progress" of the cell to the final neoplastic state. In the illustration the first stage transition is shown as resulting from 2 radiation-induced alterations (dual action). The second transition shown is spontaneous in the sense that radiation action is not required. There is a potential for any of the cells at intermediate stages to proliferate into clones thereby amplifying enormously the accumulated alterations and cells at risk for the next transition. Whether such amplification actually occurs is controversial and has only been shown conclusively for mouse skin papillomas (7).

A widely used idea to describe the effect of radiation on cell lethality and chromosomal aberrations is the dual action theory (8,9). The basis for dual action theory is that the yield of any biological endpoint requiring 2 alterations is proportional to the square of the radiation

dose in a microscopic region of space that defines the target region with the cell. The form of the dose response function, f(D), derived from this theory is:

$$f(D) = CLD + BD^2 \qquad (1)$$

or $$f(D)/D = CL + BD \qquad (1a)$$

where L is linear energy transfer, D is radiation dose and C and B are empirical constants (10). Equation 1 is derived from statistical analysis of the way radiation dose is distributed in small regions of space. It can also be derived from consideration of the track structure of ionizing radiation and the need for 2 events (9).

Cancer Incidence in Irradiated Rat Skin

The above ideas have been formulated in light of the experimental results in rat skin. Following a single dose of ionizing radiation to rat skin, epithelial and connective tissue tumors begin to appear after about 10 weeks and continue appearing at an accelerating rate until about 80-100 weeks of age after which the rate of appearance declines. The consistency of this time pattern is remarkable and is the basis for constructing time-independent dose-response relationships. A time-independent dose-response relationship is possible if the overall tumor yield function can be separated into a product of a function only of dose and a function only of time. This important idea can be expressed as follows:

$$Y(D,t) = f(D)g(t) \qquad (2)$$

where Y(D,t) is the overall cancer yield in tumors per animal, D is the radiation dose and t is the elapsed time.

The functions f(D) and g(t) require specific analytic forms and for this we rely on the multistage theory and experimental results for guidance. Experiments with irradiated rat skin suggest that g(t) is probably a power function for a large fraction of the rat's lifespan. A frequently used power function form that is compatible with the multistage theory of carcinogenesis is:

$$g(t) = k(t-w)^n, \qquad (3)$$

where t is elapsed time since exposure and k, w and n are empirical constants (4,10). This form has frequently been fitted to temporal cancer incidence data, especially epidemiological studies of cigarette smokers (10). While non-integer values of n are conceivable, consistency with the multistage model requires the use of integers. By fitting equation 3 to cancer yield data in rat skin, we estimate that w is 0 and n=2. In Figure 2 equation 3 has been fitted with w=0 and n=2 to cancer yield in rat skin exposed to single doses of 3 different types of radiation as indicated.

Proportionality of the first term in equation 1 with L, the linear energy transfer (LET), is an important implication of the dual action theory. To examine this question for cancer induction, rat skin was exposed to 3 different types of radiation with greatly different LET values; electron radiation, a neon ion beam or an argon ion beam. The latter 2 beams were generated by the Bevalac at the Lawrence Radiation Laboratory (11). The LET of these radiations were 0.34 kev/μ, 45 kev/μ and 125 kev/μ respectively. The results were a striking confirmation of the dual action theory and are given in Figure 3 which shows cancer yield per unit dose as a function of dose. These data were analyzed by fitting a line to the argon ion data by using a least square procedure. Then the line for neon ions was derived by assuming B and C remain the same and the LET changes from 125 kev/μ to 45 kev/μ. This procedure produces a line parallel to the argon ion line but shifted downward to an intercept of 0.013 tumors/rat/Gy in comparison to 0.055 tumors/rat/Gy for argon. The close positioning of the neon ion data around this predicted line is strong confirmation that Equation 1a correctly accounts for the effect of LET on cancer induction in the rat skin system. The value of the slope, B, is 0.0060 tumors/rat/Gy^2.

The same procedure incorrectly predicts the cancer yield for electron radiation. The predicted line for electrons (LET=0.034 kev/μ) from equation 1a is shown just below the line for neon ions. The y-intercept of this line is very close to 0.0 tumors/rat/Gy. The cancer yield per unit dose for electron radiation is lower and to the right of the predicted line. The

electron data are best fitted by a line with a slope of 0.0027 tumors/rat/Gy^2. The ratio of expected to observed slopes is 2.2 implying that neon and argon are 1.49 ($1.49=\sqrt{2.2}$) fold more effective than electrons for producing 2 track alterations relevant to carcinogenesis.

Another way to analyse these results, especially relevant to low dose extrapolation, is to consider the dose, D_e, where the linear and dose squared terms make equal contributions to the cancer yield. Based on $D_e = (C/B)L$ derived from equation 1, the D_e values are 8.3 Gy, 2.0 Gy and 0.05 Gy for argon ions, neon ions and electrons respectively (Table 1).

Table 1. Values for D_e in Gray.

	C	B	argon ions De	neon ions De	electrons De
high LET results	.0004	.0060	8.3	2.0	-
low LET results	-	.0027	-	-	.050

Split dose repair of radiation damage has been extensively studied for cell lethality in a variety of mammalian cells and tissues (12). The rat skin results indicate that carcinogenic alterations are subject to repair processes similar to those observed for cell lethality (13,14,15,16). A lower cancer yield was observed when electron radiation doses were split into 2 doses separated in time (Figure 4). This reduction can be interpreted to mean that the skin cells are capable of repairing part of the electron-induced damage leading to cancer. By plotting cancer yield as a function of time between doses, the repair half-time was estimated to be about 3 hrs (17,18). This result suggests that at least one event in carcinogenesis by electron radiation is repairable and that this repair can significantly reduce the risk of cancer induction. Similar methods revealed no repair of cancer induction by argon ion radiation (Figure 4).

Chronic irradiation is capable of accelerating the onset of skin cancers perhaps by acting as a promoter. When radiation doses were given weekly to rat skin for up to 1 year, the exponent of g(t) increased from 2 to 6.3; a much greater increase than would be expected if the effects of each individual dose were simply additive (Figure 5). Additivity would increase

the exponent to 3, i.e., 1 more than 2 (Equation 3). In the multistage theory the increased exponent could mean that additional stages became dose-dependent during progression or that clonal growth of one or more intermediate stages magnified the importance of a prior stage.

The evidence suggests that split dose repair continues to operate for possibly up to 52 separate exposures. This can be seen by analyzing the countervailing trends of repair and increased exponent separately. Repair tends to reduce the yield of cancer, while the high exponent tends to increase it. The accumulated dose in the chronic exposures was enormous in comparison to the single dose required to produce roughly the same yield of cancers. In spite of an exponent of 6.3, the tumor yield for chronic exposure at 1.5 Gy per week was still less than 1.0 tumor/rat at an accumulated dose of 78.0 Gy (52 exposures), while this same yield was produced by a single dose of only 15.0 Gy; a dose ratio of 5.2.

A DNA double strand break is a candidate lesion to serve as an initial alteration as specified in the model. Other common radiation- induced alterations, such as, DNA adducts, base deletions and crosslinks are permanent genetic lesions in their own right and do not need to combine with other lesions to produce genetic damage. As a test of the possibility that strand breaks might be the initial lesion in radiation carcinogenesis, we examined the induction and repair kinetics of DNA strand breaks to determine if the response pattern correlates with our knowledge about carcinogenesis in the rat skin (19). Breaks in one strand (single-strand breaks) are readily repairable, presumably correctly because of the availability of an unbroken homologous template. Breaks in both strands (double-strand breaks) are likely to result in a chromosome break which is not as readily repairable as single strand breaks, and the repair that does occur is often only partial frequently producing chromosomal aberrations (20).

Considering the possibility that 2 single strand breaks on opposite DNA strands could cause a double strand break, the kinetics of single strand break induction and repair was studied in rat epithelial DNA. Alkaline unwinding and alkaline elution were used to measure the rate of repair of DNA single strand breaks in the rat epidermis (21). The results indicated

that single strand breaks were produced in proportion to dose, and that the repair halftime was about 21 min. The latter is not very different from values found for a variety of mammalian cell lines *in vitro,* but is very different from the value of 3 hrs we found for cancer induction in rat skin. The discrepancy between repair halftimes indicates that DNA single strand breaks *per se* are not likely to be an initial alteration as required in the model. Direct measurement of double strand breaks at realistic doses has so far not proved feasible.

Another approach to identifying the genetic lesions associated with cancer progression is to identify molecular changes in the DNA of the cancers and then examine earlier neoplasias and irradiated tissue to determine if similar lesions can be found. As a first step in implementing this approach, a group of 12 well developed radiation-induced cancers were examined for activation of the *ras* and *myc* complementation groups (22). The tumors were classified histologically as follows: 4 squamous cell carcinomas, 3 poorly differentiated carcinomas (clear cell), 1 basal cell carcinoma, 1 sebaceous carcinoma, 1 sarcoma, 1 mixed carcinoma (included squamous cells) and 1 fibroma (benign connective tissue tumor). DNA was extracted from the tumors and transfected onto NIH 3T3 cells to assay for altered *ras* genes. Positive transfections (see Table 2) were found for the 3 clear cell carcinomas, the sebaceous carcinoma, the sarcoma and one squamous carcinoma. Southern blot restriction analysis revealed a rat derived restriction fragment homologous to the K-*ras* oncogene.

Southern hybridization of the original tumor DNA to the third exon rat c-*myc* probe indicated c-*myc* amplification in 10 of the 12 tumors. Neither enhanced band intensity nor restriction fragment polymorphism was seen when the DNA was probed with the first exon c-*myc* probe. These results indicate substantial amplification of the c-*myc* oncogene in carcinomas. The sarcoma was not amplified (note: subsequent analysis of additional sarcomas has failed to show c-*myc* amplification). The cause of the amplification is unknown, but it is not likely to be caused directly by radiation action (23,24,25,26,27).

Table 2. Oncogene Activation in Radiation-Induced Rat Skin Tumors.

Tumor Number	Tumor Type	K-ras	myc Amplification + Polymorphisms	myc Expression
RAD 1	Poorly Differentiated Clear Cell Carcinoma	+	+	N.D.
RAD 5	Poorly Differentiated Clear Cell Carcinoma	+	+	+
RAD 8	Clear Cell Carcinoma	+	+	+
RAD 4	Sebaceous Carcinoma (Necrotic)	+	+	N.D.
RAD 3	Basal Cell Carcinoma	-	+	N.D.
RAD 2	Well Differentiated Cornified Squamous Cell Carcinoma	-	+	N.D.
RAD 7	Squamous Cell Carcinoma	-	+	+
RAD 10	Squamous Cell Carcinoma	+	-	N.D.
RAD 12	Squamous Cell Carcinoma	-	+	N.D.
RAD 11	Mixed Histology Carcinoma (Squamous)	-	+	+
RAD 9	Sarcoma	+	-	-
RAD 6	Fibroma	-	+	+

Note: N.D. = Not Done.

Double oncogene activation (K-*ras* and c-*myc)* was found in 3 of the clear cell carcinomas and in the sebaceous carcinoma. Of 5 squamous carcinomas 4 showed c-*myc* amplification and 1 showed K-*ras* activation. The activation of the K-*ras* oncogene requires a point mutation at a specific codon, probably, 12 or 61. The radiation dose employed (12 Gy) is not likely to have produced an alteration in such a small target (one base pair) with the frequency that altered tumor DNA was actually observed as cancer incidence.

Figure 6 shows the amount of c-*myc* amplification in a large number of radiation-induced epithelial skin cancers as a function of time after initial appearance. It is not until 12 weeks that the average c-*myc* amplification reaches 3 fold; an arbitrary point separating amplified from non-amplified cancers. The data show an increased amplification with age of the tumor and support the idea that c-*myc* amplification is a late event in cancer progression.

Skin cancers were also examined for amplification of the c-*myc* oncogene by *in situ*

hybridization. The hybridization was performed with biotinylated c-*myc* probes labeled with avidin and stained with Vectastain ABC-AP (Vector Labs. Inc.). Comparisons were made with the results of Southern blots performed on DNA from the same tumors. In one instance 5 biopsies of the same squamous carcinoma permitted probing at 5 different times during cancer development. *Myc* amplification in individual cells was generally correlated with the Southern blot results.

The results of *in situ* hybridization of 7 different radiation induced cancers excised from rat skin are shown in Table 3. The density of grains in tumor sections varied with the type of tumor. The more grains observed in the tumor, the higher the c-*myc* amplification shown by Southern blotting. For example, the squamous cell carcinoma (RAD7) in which DNA amplification was increased by 20 fold exhibited the greatest number of grains in sections. The correlation is not exact, however. More grains were found in the poorly differentiated clear cell carcinoma (RAD5) than in the clear cell carcinoma (RAD8) even though the former tumor showed an amplification of 9 fold in comparison to 15 fold in the latter tumor.

Results are shown in Table 4 of *in situ* hybridization of 5 biopsy samples of the same squamous cell carcinoma (RAD 106) excised at different times in the development of the tumor. Different biotin labeled oncogene probes were used in this experiment as follows: c-*myc*, H-*ras* and K-*ras*. With the c-*myc* oncogene probe only samples 2 and 3 exhibited excess grains in comparison to control skin, and this generally agreed with the Southern blot results. With the v-H-*ras* oncogene probe, no grains were found in any tumor sections. Under close examination it was found that a specific cell type appearing small and not vacuolated exhibited c-*myc* amplification. In comparison, the non-labeled tumor cells were relatively larger and vacuolated. These data indicate that c-*myc* amplification is cell or cell cycle specific within cancers exhibiting overall c-*myc* amplification.

Table 3. C-*myc* Amplification in Radiation-Induced Rat Skin Cancers Detected by *In Situ* Hybridization Using Biotin Labeled Probe.

Number	Tumor Type	DNA amplification (Southern blotting)	Grain count* (%) (In situ hybridization)	Mean**	Adjusted mean***
RAD1	Clear cell carcinoma	>5(+)	59%	1.34	2.90
RAD4	Sebaceous carcinoma	15(+)	53%	2.07	3.70
RAD5	Clear cell carcinoma	15(+)	44%	1.57	4.70
RAD7	Squamous cell carcinoma	20(+)	62%	1.60	2.90
RAD8	Clear cell carcinoma	9(+)	28%	0.70	3.70
RAD9	Sarcoma	1(-)	3%	0.03	0.03
Control			5%	0.05	0.05

* The number of cells for which at least one grain occurred as a fraction of the total cells counted.
** Grains/cell.
*** Mean adjusted for the existence of two cell populations.

Table 4. Oncogene Amplification Detected by the *in situ* Hybridization in 5 Biopsies of a Rat Skin Cancer (Squamous Cell Carcinoma) Induced by Radiation.

Biopsy #	Time from Irradiation (week)	Tumor Size (cm^3)	Growth Rate	Oncogene Amplification c-myc	H-ras	K-ras
1	13	0.2	0.1	-	+	-
2	27	2.2	3.6	++	++	
3	33	15.0	3.2	+++	+	-
4	39	2.7	-2.2	-	-	-
5	42	1.6	-2.5	-	-	-

Grains were observed with a microscope and scored as follows:
(+) :low grain count.
(++) :intermediate grain count.
(+++) :high grain count.
(-) :no grains

1.2 *Discussion of Results*

The above results can be explained by assuming electron radiation produces an initial repairable alteration that interacts with a second similar alteration to form an irreparable genetic lesion. The latter lesion advances a cell 1 stage in the progression to cancer. One or

more additional stage transitions may be necessary to complete the conversion to a cancer cell, and the latter transitions may occur many cell divisions after the initial lesion is formed. There is substantial support for initial action followed by late conversion from studies with chemical carcinogens in the mouse skin and rat liver (28,29). These ideas generally encompass what is known as cancer progression. This type of progression may occur naturally without the need for action by the radiation.

The stages in the multi-stage theory of carcinogenesis are considered to be non-repairable (10). If stages were repairable, one would expect a reduction of cancer yield at lower dose rates, but such reductions have not generally been observed with chemical carcinogens. For ionizing radiation, on the other hand, cancer yield is reduced at lower dose rate. By these definitions repairable alterations can not be the basis for a stage transition in the progression to cancer. Such transitions require a non-repairable genetic lesion transmissible to daughter cells. As applied to carcinogenesis, the dual action hypothesis postulates that 2 repairable molecular changes are the starting point and that an interaction between them produces an an irreversible lesion that moves the cell to the next stage of progression to cancer. Altered cells may progress even further by acquiring additional lesions (30,31,32). Interactions between primary events are envisioned to proceed quickly if they are in close geometrical and temporal proximity. A plausible candidate for the primary alteration is a double strand break in the deoxyribophosphate strand structure.

The dose-response relationship in equation 1 can be derived from the track structure of ionizing radiation and the 2 event assumption. Assume that the distribution of carcinogenically-relevant alterations in the nucleus is similar to the distribution of primary ionizations. If the LET of the radiation is low, many individual tracks are necessary to produce a given dose, and the biological alterations are likely to occur in different particle tracks. Since events in different tracks are independent, the probability of two events occurring within an interaction distance is the product of the individual probabilities. With events proportional to dose, the yield of interactions between events in different tracks is proportional to dose

squared which gives the second term in equation 1: BD^2. Repair is observable because events in different tracks can be separated in time.

At higher LET values the number of tracks necessary to produce a given dose declines inversely proportional to LET. At very high LET values, e.g., 100 kev/μ or higher, hundreds of rads can be delivered by only a few tracks per nucleus. If only a few tracks pass through a nucleus, interacting events are likely to be linked in the same radiation track. The chance of an interaction between events in the same track is proportional to the number of tracks, i.e., dose, and inversely proportional to separation, i.e., LET, which gives the first term in equation 1: CLD. Repair is not observable because events in the same track occur closely in time leaving no time for repair.

The approach to radiation carcinogenesis outlined here is overly simplified in that it neglects a number of potentially important factors, such as, the cytotoxic effect of the radiation and the likelihood that a variety of local (growth factors) or systemic factors (hormones) may modify the expression of neoplastic and potentially neoplastic cells. Certainly, cytotoxicity cannot be ignored at doses above the peak tumor yield where further dose increases lead to unregenerated tissue destruction and fewer tumors, accordingly the model can only be applied below the peak yield dose.

It is interesting that the cancer yield in rat skin is not affected by cell lethality at intermediate radiation doses. At high doses where proliferative repopulation is incomplete, cancer incidence is clearly reduced by the death and non-replacement of cells at risk, but no reduction is observed at doses where repopulative regeneration is complete. One possible explanation of this finding is that carcinogenically-altered cells participate in proliferative repopulation.

2.0 *Cell Cycle Kinetics of Irradiated Rat Epidermis Determined by Double Labeling and Double Emulsion Autoradiography*

The purpose of these studies was to determine how ionizing radiation affects the epidermal cell kinetics following a standard proliferative stimulus. The loss of keratinized cells and

keratin from the skin surface causes an increased rate of cell proliferation in the basal cell layer (33-38). This property was used to assay the radiation damage to the basal cells by determining the magnitude of the proliferative response at different doses of ionizing radiation. The "method of labeled mitoses" has been used extensively to measure the cell cycle of proliferating populations of cells by direct estimation of the durations of the cell cycle phases (39,40). Unfortunately the method is tedious to use in a slowly dividing tissue, such as epidermis, because of the low frequency of mitotic figures. This difficulty can be overcome to a considerable extent by replacing the "mitotic window" with the considerably larger "S-phase window" through the use of a double isotope technique and skin biopsies (Figure 7). This approach provides what by analogy could be called a "labeled S-phase" curve, and gives similar phase and cycle time information as the more conventional labeled mitosis curve (41-46).

The conventional labeled mitosis curve for untreated rats is shown in Figure 8. An injection of vinblastine 4 hrs before sacrifice was used to increase the number of mitoses. The percentage of mitoses labeled at 4 hrs and 8 hrs was 46% and 98%, respectively, and these data are not shown in Figure 8. The value at 24 hrs was zero out of a total of 250 mitotic figures, and after that the percentage of labeled mitoses varied between 1.2% to 3.5% with an average value of 2.2%. The curve shown is the one that would be expected if the cycle contained a G_0-phase and if the constant phase time (pre-S, S, G_2 and M) were 40 hrs (37).

The ^3H labeling index of the basal cells irrespective of the presence of ^{14}C is shown in Figure 9. At 0 Gy there was a marked increase by 24 hrs indicating that cells were entering S-phase as a result of the stripping only after a delay of this length of time. After some fluctuation the points settle to a value estimated at 35 hrs and beyond to be 11.8%. At 10 Gy the increase is delayed to 42 hrs then averages 5.3%. At 25 Gy the increase is further delayed to 54 hrs, and the average value is 6.6%, although the fluctuations are relatively large. If the time of increase is arbitrarily established as the time where the index first exceeds 4%, 18 hrs, 32 hrs and 53 hrs are the times of the first cells entering S-phase after stripping at 0

Gy, 10 Gy and 25 Gy, respectively.

The ^{14}C labeling index for the basal cells irrespective of the presence of ^{3}H is shown in Figure 10. The data generally lie within the range of 2% to 5%, without an obvious increasing or decreasing trend. There are no significant differences between the average values of 3.2%, 3.6% and 3.7% at 0 Gy, 10 Gy and 25 Gy, respectively.

The doubly labeled cells as a fraction of the ^{3}H-labeled cells, i.e. the labeled S-phase curves, are shown in Figure 11. Irrespective of the radiation there was a delay of about 42 hrs to 53 hrs after the initial ^{14}C-thymidine injection before significant numbers of doubly labeled cells appeared. Beyond 42 hrs the values fluctuate somewhat, and the averages of 2.8%, 2.8%, and 3.7% at 0 Gy, 10 Gy and 25 Gy, respectively, are not significantly different. A few points are missing as a result of defective autoradiographs.

The doubly labeled cells as a fraction of the ^{14}C labeled cells are shown in Figure 12. As in the labeled S-phase curves doubly labeled cells were first seen at 42 to 53 hrs. Unlike the labeled S-phase curve the average fraction at 0 Gy was significantly higher (11.8%) than at either 10 Gy or 25 Gy which were not significantly different than each other at 3.5% and 4.0%, respectively.

The total number of Feulgen positive cells per unit distance along straight, 50 μ segments of epidermis was determined on the sections. The results, expressed as percentage of the number of cells at 18 hrs, are shown in Figure 13. At 0 Gy the number of cells was essentially constant. At 10 Gy and 25 Gy there was a steady decline with a slope of about 0.5%/hr (12%/day) until the end of the experimental period at 124 hrs.

Double emulsion autoradiography for distinguishing ^{14}C labeled cells, ^{3}H labeled cells and doubly labeled cells is not used frequently, so its reliability needs to be examined. Table 5 gives average grain and track counts within the nuclear area in the first emulsion for each isotope. The data in Table 5 shows that ^{14}C produced very few grains in the first emulsion in comparison to ^{3}H. This was achieved by producing a high ratio (estimated at 50:1) of ^{3}H to ^{14}C in the tissue and by using a thin first emulsion. The nitrocellulose layer stopped the

^{3}H betas from reaching the second emulsion and provided a microscopically clear demarcation between emulsions.

2.1 *Discussion of Results*

The use of multiple biopsies helps to reduce individual variation in the experiment and to conserve isotopes and animals, but local proliferation rates may be affected by wound healing at distant biopsy sites. To minimize this possibility, at least 4 mm of clear skin was left between biopsy sites. Results have been reported indicating that proliferative wound repair does not extend beyond about 3 mm and is concentrated in the first 1 mm from the edge of the wound. To confirm this an experiment was done to measure the pulse labeling index following an intraperitoneal injection of ^{3}H-thymidine as a function of distance from a biopsy at various times. Two rats were used at each point and the results are shown in Table 6. These data show that the biopsy had no effect on the L.I. beyond 3 mm except for a slight increase at 48 hrs, which was small and non-persistent compared to that caused by stripping the skin surface.

The nitrocellulose layer caused a spreading of the ^{14}C grain pattern in the second emulsion such that most of the grains (and tracks) occurred within a diameter of about 2 or 3 nuclear diameters, i.e. about 12 μ or 18 μ. Although this would be a relatively poor resolution in single isotope autoradiography, in practice it was acceptable because the grains and tracks were arrayed symmetrically in a pattern centered on the labeled cells. Moreover ^{14}C-labeled cells were relatively infrequent so that labeling patterns rarely overlapped. Resolution was sufficient in most instances to decide whether ^{14}C-labeled cells were in the basal or superficial layer.

It is interesting to note that in spite of a substantial increase in the rate of cells entering DNA synthesis at 0 Gy, there was no increase in the total number of cells as determined by Feulgen positivity (Figure 13). The implication of this observation is that rate of differentiation must have increased after the stripping in order to maintain a steady state of total cell number (47-51).

Another interesting point is that the radiation seemed to have an equivalent lethal effect on the ^{14}C-labeled cohort as on the population as a whole. At a radiation dose where the total cell number was eventually reduced to nearly one-half of control, the proportion of ^{14}C-labeled cells remained fairly constant and about equal to the value in controls, i.e. ^{14}C-labeled and unlabeled cells were lost equally (Figure 10). Since most of the ^{14}C-labeled cohort would have been in the G_1-phase at the time of irradiation, some of the observed cell loss must have been the result of the loss of G_1 cells. The latter observation implies that a substantial fraction of the observed cell loss was differentiative loss not compensated by proliferative replacement. It is also interesting to note that there was no preferential loss of non-^{14}C-labeled cells as might be expected if the cells were dying preferentially at mitosis.

The results are consistent with a non-uniform cycle time. If the cycle time were uniform, a conventional labeled mitosis curve should drop to 0 after the first peak and not rise again until a second peak occurs in the vicinity of the mean cycle time. Based on the formulae $L.I.=K_pT_s$ and $T_c=1/K_p$ the cycle time, T_c, is estimated to be about 286 hours (L.I.=.035, T_s=10 hr). The constant level of about 2.5% seen in the labeled mitosis curve after about 40 hours (Figure 8) implies that the cycle times are not uniform but are widely distributed with a minimum cycle time of about 40 hours. In the uniform cycle time model, stimulating proliferation by stripping would have reduced the cycle time to about 66 hours. No evidence of a second peak in the vicinity of 66 hours was found in the present experiment (see Figure 11). A wide distribution of cycle times is consistent with the existence of a G_o-phase from which cells are released randomly (37,52,53,54,55). After release from the G_o phase, cells enter a uniform duration phase, consisting of pre-S-phase, S-phase, G_2-phase and mitosis.

The main effect of the radiation was to reduce the number of cells being released into the S-phase (Figure 3). The radiation did not affect the minimum time at which ^{14}C-labeled cells first appeared in significant numbers in S-phase (Figures 11 and 12), and it had no effect on the proportion of ^{14}C-labeled cells entering S-phase (Figure 12). This implies in the G_o model that the radiation suppressed the increase in the rate at which cells were leaving the

G_0-phase but had no, or only a minor, effect on the length of the presynthetic phase and the S-phase (56,57,58). Thus, the delay in the increase in the ^3H labeling index following irradiation (Figure 9) can be explained as the result of a delay of irradiated cells in leaving the G_0-phase rather than a change in the time required to pass through the presynthetic phase and S-phase.

Support for the random triggering assumption of the G_0 model can be found in Figure 11. For cell populations in widely different states of proliferation as indicated by the ^3H labeling index (Figure 9), there is no difference in the proportion of ^{14}C-labeled cells entering S-phase. This is exactly what would be predicted by the random triggering model, i.e. once a cell enters the G_0 phase its chance of leaving is independent of when it entered. The ^{14}C-labeled cells enter G_0 as a cohort and yet are equally likely to be triggered into S-phase as the unlabeled cells. This is another way of saying that the triggering of cells into the S-phase is random; a key assumption of the G_0 model. This can also be seen from the data in Figure 12 which indicates the proportion of the ^{14}C-labeled cells that enter the S-phase at the various doses. These data indicate that the ^{14}C-labeled population behaves very similarly to the overall population (Figure 9) in the proportion of cells that enter S-phase under the various conditions employed in the experiment.

In spite of the relatively large radiation doses, surviving cells retain a considerable proliferative capacity. The data in Figure 9 show that, while the number of Feulgen positive cells is decreasing (Figure 12), the rate at which cells are entering the S-phase is increasing, although at a lesser rate than the unirradiated controls. This implies that some cells that survive the radiation are still able to proliferate. The increase in proliferation in the irradiated skin is so delayed that the stripping alone or the stripping in combination with radiation-induced depletion could have been the stimulus (59,60).

3.0 *Oncogene Activation Detected by In Situ Hybridization in Radiation-Induced Rat Skin Tumors*

It is widely accepted that exposure to radiation can induce tumors in many organs and species (61). The mechanism responsible for radiation carcinogenesis has been studied and several general hypotheses have been proposed (62,63). The most common one is the " dual radiation action theory ", which states that sublesions are produced depending on the pattern of energy transfers to the cell, and that these sublesions can interact in pairs to produce lesions which in turn determine the observed effect (63). Presumably at least two radiation-induced genetic alterations are required in tumor development. Ionizing radiation can cause a variety of lesions in DNA, including base modification, single and double strand breaks, sugar damage and DNA-DNA or DNA-protein crosslinking (64). How radiation-induced DNA damage initiates a normal cell and subsequently stimulates tumor cell proliferation are major issues for understanding radiation carcinogenesis. Carcinogenesis is considered to be a multistage process involving initiation, promotion, and tumor progression (65,66). The heritable nature of tumor- related-alterations makes it necessary to examine the incidence of genetic alterations in different stages of tumor development. Recently the demonstration of specific oncogene activation in radiation-induced cancer cells has been responsible for an increased understanding of the molecular mechanisms of radiation carcinogenesis (67).

Rat skin exposed to ionizing radiation exhibits a variety of tumor types, including squamous carcinomas, basal cell carcinomas, sebaceous cell tumors and sarcomas (68). The dose-response relationship in rat skin cancers induced by ionizing radiation is well established, and follows, like the effect of radiation on cell lethality and chromosomal aberrations, a linear-quadratic pattern (62,69). Rat skin tumors induced by ionizing radiation provide an excellent model for studying oncogene activation during tumor progression. Tumors are visible early and are available to be excised or biopsied. By taking a series of biopsies from a growing tumor, it is possible to examine the activation of oncogenes during the development of individual tumors (70).

Detection of oncogene amplification in rat skin tumors induced by radiation has contributed valuable information for understanding the connection between initiation of carcino-

genesis and activation of oncogenes. The results from Southern blot hybridization of the Bam H1 digested tumor DNA with a human c-*myc* third exon probe revealed amplification of the c-*myc* oncogene in 10 of 12 tumors. The *myc* gene was amplified 5 to 20 fold based on densitometric analysis (71,72). The result of Southern hybridization of tumor DNA from serial biopsies of an individual tumor showed that the c-*myc* amplification was correlated with both the size and growth rate of the tumor (73). Other studies have indicated that c-*myc* amplification is more likely a late event rather than a early event in carcinogenesis (70). Recent evidence indicates that c-*myc* expression is involved in controlling cell proliferation (74,75).

The purpose of the present study was to make use of *in situ* hybridization (a) to provide information on c-*myc* amplification of cells from cancers with differing degrees of c-*myc* amplification as shown by Southern blotting and (b) to examine cell proliferation and c-*myc* amplification in rat epidermal cells at early times after exposure to ionizing radiation. *in situ* hybridization has provided an efficient tool to localize a specific nucleic acid sequence in tissue sections (76,77,78,79,80,81). The technique is based on the formation of a highly specific hybrid between an appropriately labeled nucleic acid probe and its complementary sequence in the specimen. This technique can yield both molecular and morphological information about individual tumor cells. The use of a biotinylated c-*myc* probe and an avidin-biotinylated alkaline phosphatase detection system has the following advantages over the use of a radioactive probe: rapid detection, improved microscopic resolution, and avoidance of a radiation hazard (82,83,84).

A dry ulceration was noted in rats exposed to 20 Gy of ionizing radiation at day 7 and beyond. No evidence of tissue damage or ulceration was seen in rats exposed to 0 Gy or 10 Gy at any time point.

A variety of rat skin tumors were hybridized with a biotinylated c-*myc* third exon probe *in situ*. Figure 1 (A-D) shows photomicrographs of tumor sections after *in situ* hybridization and illustrates the microscopic view of the 5 biopsy samples from a single squamous cell

carcinoma. As indicated by the symbols, T1(2)-T1(5), each photomicrograph represents different stages of tumor development. Red grains were found in several tumor sections in which biotin labeled oncogene probe was employed. The grains are considered to be a granules of stain associated with the probe hybridized to amplified oncogenes. The background grain count in normal tissue sections was very low (0.05 grains/cell) indicating that the single copy gene was not detectible by the present methods.

The number of grains in tumor tissue was dependent on both the type of tumor and the stage of tumor progression in 5 biopsy samples. The results indicate that certain types of cancers and certain stages in cancer progression exhibit many grains. The number of grains on tumor slides is presumably proportional to the magnitude of oncogene amplification. The grains were found almost exclusively over the nucleus of tumor cells. In some cells the grains were distributed randomly within the nucleus, but in others the grains were localized near the nuclear membrane. Very few grains were found over the cytoplasm or over extracellular spaces.

The pattern of grain distribution helps to confirm that the grains were the result of the probe binding to the DNA of nuclear oncogenes. The use of RNase before hybridization did not change the distribution of grains in tumor sections, however the use of DNase before hybridization eliminated all the grains in the sections, which was a second indication that the probe hybridized primarily to DNA and not RNA.

Shown in the Table 5 are the results of *in situ* hybridization of the c-*myc* probe to 7 different radiation induced cancers excised from rat skin. The number of grains per cell varied with the tumor type, but correlated generally with the c-*myc* amplification as found on Southern blots. But the grain count did not always match the Southern blot results quantitatively. For example, RAD5 showed almost twice the amplification of RAD1 and yet the number of grains per cell of RAD5 was nearly half that of RAD1. More grains were found in the clear cell carcinoma (RAD8) than in the poorly differentiated clear cell carcinoma (RAD5); even though the former tumor had a low c-*myc* amplification factor (9x) and the

latter one had a high c-*myc* amplification factor (15x). Examination of the tumors revealed that only specific cell types within the tumor sections showed c-myc_ related grains. The c-*myc* positive cells were relatively small and not vacuolated in comparison to the c-*myc* negative cells in the same tumor. No grains were found in a sarcoma which was also negative by Southern blot analysis.

The distribution of grains among the cells was not consistent with a Poisson distribution; there were consistently more cells than expected with no grains. In the most extreme example, RAD 8 exhibited 80% cells with no grains when the expectation based on a random distribution was less that 10%. One intrepretation of this finding is that the cancers consist of at least 2 subpopulations of cells; one labeled randomly showing amplification and one not labeled and lacking c-*myc* amplification. By analyzing the results in terms of 2 subpopulations, we have arrived at adjusted mean grain counts and percentages not amplified as indicated in Table 5. For purposes of the analysis, it was assumed that only 2 subpopulations existed; 1. a c-*myc* positive subpopulation distributed randomly and 2. a c-*myc* negative subpopulation exhibiting no signal by *in situ* hybridization and no amplification. This analysis indicates that on average about 48% (33% to 70%) of the cancer cells are part of a c-*myc* negative population.

Shown in the Table 6 are the results of *in situ* hybridization to 5 biopsies of a squamous cell carcinoma (RAD 106) obtained at different times during tumor development. The tumor developed sequentially from T1(1) to T1(5), and represented growth followed by regression as indicated. Several biotin labeled oncogene probes, including, c-*myc*, v-H-*ras* and v-K-*ras* were used in the 5 biopsy experiment. For the c-myc_ probe, only samples T1(2), T1(3) showed grains; the grains in T1(3) were greater in number than in T1(2). No grains were observed in tumor sections without denaturing the DNA which confirms that the probe is specific to single stranded DNA. Using the biotinylated rat v-H-*ras* probe, grains were found in tumor sections T1(1), T1(2), and T1(3). The number of grains was low in T1(1), high in T1(2) and medium in T1(3). The pattern of amplification in tumor development is similar

between v-H-*ras* and c-*myc*. With the biotinylated v-K-*ras* probe, no grains were found in any tumor sections indicating that this oncogene was not amplified.

Normal skin tissue sections were prepared at 1, 7, 14 and 21 days after exposure to 0 Gy, 10 Gy or 20 Gy of electron radiation. *In situ* hybridization with the c-*myc* third exon probe revealed no c-*myc* amplification in any of these tissue sections including irradiated and unirradiated. Hyperplasia of epidermis was seen in these sections.

Another group of rats was used to assay epidermal cell proliferation after radiation exposure. Rats were irradiated with 0 Gy, 10 Gy or 20 Gy. Following irradiation the rats were injected with 1.0 fci/g ^{3}H-thymidine at 1, 7, 14 and 21 days. Based on counting cells on autoradiographs, labeling indices were obtained for the epidermis and are shown in Figure 2. The percentage of labeled cells is proportional to cell proliferation rate at the time of exposure to ^{3}H-thymidine. On the first day no significant difference was seen between 0 Gy and 10 Gy, but a large increase of labeled cells at day 7 in 10 Gy group occurred, followed by a decline at day 14 and day 21. After day 7 the epidermal layer of skin exposed to 20 Gy could not be found, presumably due to the cytotoxicity of this dose. The total cell count in Figure 3 shows a similar pattern as the labeling index, i.e. an increase at day 7 followed by lesser decreases at days 14 and 21.

3.1 *Discussion of Results*

The results here provide evidence for the amplification of the c-*myc* oncogene in specific cells in several different types of rat skin carcinomas induced by ionizing radiation. A reasonably good correlation was found between the methods of Southern blotting and *in situ* hybridization as measures of c-*myc* amplification in these cancers. In five biopsy samples from a single cancer, the observation that c-*myc* oncogene amplification was correlated with stages of tumor development was also consistent with results from the Southern blotting experiments. There were small quantitative differences in the pattern of c-*myc* oncogene amplification in the different stages of tumor development based on these 2 methods. By Southern hybridization analysis, the c-*myc* copy number was the greatest in the second biopsy,

T1(2), and decreased in subsequent ones, while by *in situ* hybridization the grain count was greatest in the third biopsy, T1(3).

A major finding was the co-amplification of v-H-*ras* and c-*myc* oncogenes in the 5 biopsy samples by *in situ* hybridization. The same cancer analyzed by Southern blotting indicated minor amplification of v-H-*ras* (maximum 2.0 fold). Localization of the v-H-*ras* amplication to a subpopulation of cancer cells may explain this discrepancy. There was evidence of co-amplification in some of the biopsy samples, and yet the pattern of H-*ras* amplification was slightly different than that of c-*myc*. It is a reasonable supposition that c-*myc* amplification is involved in radiation-induced carcinogenesis, but it is doubtful that c-*myc* amplification is an early event in tumor development.

The rat epidermis at very early times, i.e., days 1, 7, 14 and 21 after exposure to ionizing radiation did not show significant c-*myc* amplification when compared to tumor tissue that served as a positive control. The fact that the proliferation of epidermal cells showed a large increase at day 7 in the absence of c-*myc* amplification indicates that c-*myc* amplification is not likely to be involved in the control of proliferation associateed with radiation wound regeneration fo epidermal cells.

A morphologically distinct subpopulation of cancer cells was found that exhibits no c-*myc* amplification. The size of this subpopulation varied from 33% to 70% in different cancers. Microscopic examination showed that the amplification occurred preferentially in specific tumor cells characterized as smaller and relatively unvacuolated in comparison to c-*myc* negative cells. These cells are presumably involved in tumor growth, although this remains to be demonstrated. In many cells grains were concentrated toward the periphery of the nucleus indicating localization of c-*myc* DNA near the nuclear envelope. This finding needs to be confirmed in other cells, but consideration of this distribution pattern may contribute to understanding oncogene action.

The results here confirmed that the application of *in situ* hybridization using biotinylated oncogene probes in tumor sections was a reliable method to investigate oncogene activities in

carcinogenesis and made possible the observation that oncogene activation is cell specific within the developing tumor. The use of the biotin labeled probe greatly increased the detection of c-*myc* amplification in comparison to the use of a radioactive probe. The biotin method is relatively rapid in contrast to the long exposure time of the autoradiographic method. Initially the loss of tumor tissue from the slide was a difficult problem due to the high temperature treatment and tiny contact area of the tissue on the slide. Both adhesion of tumor tissue to the slide and a smooth coverslip are important requirements for successful *in situ* hybridization. Polylysine coated slides and siliconized coverslip using Sigmacote proved to be an efficient way to keep the tumor tissue on the slide.

Specific oncogene activation in tumor cells has attracted much attention recently (85,86,87,88). Different approaches have been applied to explore the correlation between specific oncogene activation and tumor development. The radiation-induced rat skin carcinogenesis model has been extensively used to examine oncogene activation. Some rat skin tumors tested were positive in the NIH/3T3 transfection assay, implying activation of the *ras* oncogene family. Southern analysis of the tumor DNAs revealed evidence for c-*myc* gene amplification by 5- to 20- fold. The amplification of c-*myc*, H-*ras* or K-*ras* was found to be associated with an increase in tumor size and c-*myc* amplification was associated with an increase in growth rate. Amplification of c-*myc* was found in other work to be a late-stage event in cancer development. These results indicate that *myc* and *ras* genes play unique roles in the growth and development of radiation-induced rat skin tumors.

Table 5. C-*myc* Amplification in DNA from Radiation Induced Rat Skin Tumors Detected by *in situ* Hybridization Using a Biotinylated c-*myc* Third Exon Probe.

No.	Tumor Type	DNA Amplifications (Southern blotting)	Labelled Cells[1] (%)	Mean[2]	Adjusted Mean[3]	Cells not amplified (%)
RAD1	Clear cell carcinoma	5x	60	1.34	2.06	35
RAD4	Sebaceous carcinoma	15x	53	2.07	3.83	46
RAD5	Clear cell carcinoma	15x	44	1.57	3.49	55
RAD7	Squamous carcinoma	20x	62	1.60	2.38	33
RAD8	Clear cell carcinoma	9x	20	0.70	2.33	70
RAD9	Sarcoma	1x	3	0.03	0.03	-
Control			5	0.05	0.05	-

[1] The percentage of cells in which at least one grain occurred.

[2] The unit is grains/cell.

[3] The mean is adjusted for the existence of 2 cell populations (see text).

Table 6. Oncogene Amplification Detected by *in situ* Hybridization in Five Biopsy Samples from a Squamous Cell Carcinoma Induced by Ionizing Radiation in Rat Skin.

Biopsy #	Time after irradiation (week)	Tumor size (cm^3)	Growth rate[1]	Oncogene amplification[2] c-myc	H-ras	K-ras
1	13	0.2	0.1	ND	+	ND
2	27	2.2	3.6	++	+++	-
3	33	15.0	3.2	+++	++	-
4	39	2.7	-2.2	-	-	-
5	42	1.6	-2.5	-	-	-

[1] The unit is percentage area change per day.

[2] The grains were scored as follows:

(+): low grain count (1.0/cell).

(++): intermediate grain count (>=1.0/cell, <2.0/cell).

(+++): high grain count (>=2.0/cell).

(-): no grains.

ND: no data.

4.0 *Retinoblastoma Gene Polymorphisms and Amplification of the c-myc Oncogene in Radiation-Induced Rat Skin Tumors as a Function of LET*

Restriction fragment length polymorphisms (RFLPs) of the retinoblastoma (Rb) gene in rat skin cancers induced by electrons or neon ions.

As a test of the suppressor gene inactivation hypothesis, the DNA of rat skin cancers induced by different types of ionizing radiation (electrons and neon ions) was examined for evidence of RFLPs in the Rb gene. CD rats are an outbred population that has been maintained by the breeder (Charles River Farms, Inc.) for many years. To investigate the possibility of spontaneous population polymorphisms of the Rb gene in this population, DNA from 12 special controls selected from different maternal and paternal parentage, and 20 regular controls (as normally supplied by the breeder) were analyzed for Hind III or Eco RI RFLPs. Southern blots of DNA extracted from the kidneys of 10 regular controls digested with Hind III or Eco RI is hybridized to the human Rb c-DNA probe. Multiple lanes with control rat DNA show essentially identical patterns indicating the lack of Rb population polymorphism for Hind III or Eco RI. Additional Southern blots indicated no evidence of Hind III population polymorphism in a total of 32 control DNA samples.

Southern blots of Hind III digested DNA from normal human placenta and 16 rat skin cancers induced by neon ions and hybridized to the human Rb c-DNA probe show band differences estimated quantitatively by scanning densitometry of the gel films. Densitometric results were confirmed by visual inspection. The Hind III RFLPs in the cancer DNA include a new band at 3.2 kb; a new band at 11 kb in; and a new band at 15 kb. The restriction fragment pattern for 2 tumors showed no differences from the pattern in control DNA. The results in 4 tumors were inconclusive because of inadequate gel loading or DNA degradation.

Southern blot of Hind III digested DNA from normal human placenta and 16 rat skin cancers induced by electron radiation and hybridized to the human Rb c-DNA probe indicate that the RFLPs of electron-induced cancers differ from the RFLPs seen in the DNA from neon ion-induced cancers. The electron-induced RFLPs include new bands at 18.4 kb and/or 10 kb in 7 tumors. The pattern for 4 tumors showed no differences from the control pattern. Results for 5 tumors were inconclusive because of sample degradation or inadequate gel loading.

A Southern blot of Eco RI digested DNA from normal human placenta and 11 rat skin

cancers induced by neon ions were compared. Eco RI Rb RFLPs in the DNA of neon ion-induced cancers include a new band at 5.3 kb in 4 cancers; and missing or weak bands at 2.5 kb and 10 kb for 1 cancer. The pattern for 1 tumor showed no differences from the control pattern. The results for 5 cancers were inconclusive because of sample degradation or inadequate gel loading.

A Southern blot of Eco RI digested normal human placenta and DNA from 17 cancers induced by electron radiation were compared. Eco RI Rb RFLPs include new 17 kb bands for 4 cancers and a missing or weak band at 7.0 and a new band at 3.4 for 3 cancers; missing or weak 4.3 kb and 8.0 kb bands for one cancer; and loss of a 4.3 kb band and gain of a 3.2 kb band for one cancer and gain of 1.3 kb and 2.0 kb bands for another. The patterns for 3 cancers showed no differences from control, although possible new bands were noted in the region of 1.9 kb in 2 cancers. Results for 4 cancers were inconclusive because of sample degradation or inadequate gel loading.

As indicated in Table 7 showing summary results for neon ions and electrons, cancers were selected for study at various times after irradiation. A small sample of each cancer was excised and processed for histological diagnosis. The cancers were generally large and invasive at the time of sampling which varied from 27 to 114 weeks after irradiation. The neon ion-induced tumors occurred in rats that received single exposures of 4 to 16 Gy of radiation dose, while all but 1 of the electron-induced tumors were taken from rats that received 25 Gy. The distribution of different histological types of tumors, tumor sizes, tumor occurrence times and tumor excision times were comparable for electron radiation and neon ions. For each cancer designated with an + in columns 2 and 6 of Table 7, RFLPs were found on the Southern blots. The results are reported either as new bands or loss of bands in comparison to the control patterns.

The Hind III polymorphisms in neon-induced cancers involve new bands at 11 and 3.2 kb, while new bands occurred at 15.4 and 10 kb for electron-induced cancers. The Eco RI polymorphisms involve new or missing bands at 10 kb, 5.3 kb and 2.5 kb for neon ion-

induced cancers and at 17 kb, 8.3 kb or 2.4 kb for electron-induced cancers. Gel loading relative to control was estimated by densitometry of photographs of ethidium bromide stained agarose gels illuminated with UV radiation.

Of 23 cancer DNAs with adequate Hind III patterns, 17 showed some evidence of RFLPs. Of the 9 lanes with weak or missing bands (possible total Rb deletions), 6 lacked concordance with the corresponding Eco RI result and the remaining 3 could be explained by inadequate gel loading or apparent DNA degradation. Thus none of the weak patterns could be confirmed as possible deletions in this sample of tumors. Out of a total of 16 cancers adequately analyzed with both Hind III and EcoRI, 11 (69%) showed concordant results with both enzymes. Out of 26 cancers for which at least 1 adequate restriction enzyme pattern was available, 21 (81%) showed evidence of RFLPs in the Rb gene, including 7/9 squamous carcinomas, 7/7 basal cell carcinomas, 5/8 sarcomas, 1/1 clear cell carcinoma and 1/1 fibroma. For summary purposes the clear cell carcinoma is included with basal cell carcinomas and the fibroma is included with sarcomas.

Table 7. Summary of RFLP pattern and other characteristics of rat skin cancers induced by neon ions or electrons. Symbols are as follows: + = positive RFLP, - = negative RFLP, I = inadequate gel pattern, 0 = not tested, BCC = basal cell carcinoma, SCC = squamous cell carcinoma, SAR = sarcoma, CC = clear cell carcinoma, F = fibroma.

Neon ion-induced tumors					Electron-induced tumors				
1	2		3	4	5	6		7	8
Tumor #	Southern blot results		Hist-ology	Excision time (wks)	Tumor #	Southern blot results		Hist-ology	Excision time (wks)
	Hind	Eco				Hind	Eco		
319	-	+	BCC	90	101	I	+	SCC	50
331	-	+	SAR	90	102	+	+	SCC	55
333	+	+	SAR	93	104	-	-	SAR	45
340	I	0	SAR	93	106	-	-	SCC	27
349	I	I	SAR	82	115	+	+	BCC	55
350	+	I	SAR	82	117	I	+	SCC	94
351	+	0	SAR	60	133	+	+	SCC	68
405	+	I	BCC	82	134	-	-	SAR	68
388	+	+	SCC	74	135	+	+	SAR	69
389	+	+	BCC	73	136	+	+	BCC	68
390	+	0	BCC	73	141	+	+	CC	94
392	I	0	SAR	73	156	-	I	SAR	61
395	+	-	BCC	73	157	I	I	SAR	61
383	+	I	SCC	68	158	I	+	SCC	61
384	+	0	SCC	68	159	+	+	F	61
399	I	0	SCC	81	181	0	I	BCC	94
408	0	I	SCC	68	170	I	I	BCC	78

These results indicate a high incidence (81%) of RFLPs in the DNA of these cancers and a difference between the restriction patterns of DNA from electron-induced cancers in comparison to neon ion-induced cancers. The evidence presented can not rule out the possibility that the observed RFLPs are the result of mutations at restriction sites. However if restriction site mutations were occurring in tumors, mutations at non-restriction sites should also be occurring with about the same frequency per site. Restriction sites outnumber non-restriction sites by a wide margin, and yet only 7 of 26 (27%) adequately tested cancers exhibited normal Hind III or Eco RI restriction patterns indicating that the upper limit of the incidence of restriction site mutations is much lower than the incidence of major polymorphisms. Further study will be needed to establish whether the Rb RFLPs reflect gene damage sufficient to inactivate the gene and whether intragenic deletions are involved.

Cancers generally contain some non-cancer cells, including white blood cells, fibroblasts and endothelial cells, so it would not be surprising to find weak bands at a location that may have been totally deleted in the cancer DNA. Several of the tumor lanes show weak bands rather than total band loss at positions of bands in the controls. Weak (generally about 20% of control) bands are most likely normal cell contamination, but complicate the inter- pretation of the complex Rb restriction patterns. A restriction map of the rat Rb gene is not currently available, so it is not possible to compare the observed banding pattern with expectations. The number of bands in the rat DNA is greater that the number in the human control DNA and some of the extra bands could be artifactual from the use of a cross-species probe. Nevertheless the banding pattern in the rat DNA is quite reproducible in a large number of control rats as well as in cell lines derived from normal skin and respiratory cancers of different strains of rats (data not shown).

Because radiation-induced deletions in DNA are often large and can occur anywhere in a gene or chromosome, it is somewhat surprising that no unequivocal instances of total Rb deletions were found among the 34 cancers tested in these experiments. Perhaps critical genes reside close to the Rb gene in the rat making large deletions that include flanking sequences lethal to the cells. Four of 11 electron-induced cancers exhibited a Hind III polymorphic pattern that included the appearance of a new band at 17 kb. The consistent location of the new band suggests possible clustering of the associated breakpoints. While the Rb polymorphisms seen here are not unlike those found for other genes, eg. HPRT, inactivated by radiation, selection operating on cancer cells could alter the distribution or type of RFLPs in comparison to what occurs in genes selected differently. Population polymorphisms in the Rb gene described in humans usually involve mutations at restriction sites (40). However such Rb polymorphisms are infrequent and no RFLPs of any type were detected in a sample of 32 rats drawn from the CD-1 population.

One electron-induced tumor was a fibroma, which is a benign connective tissue tumor. Fibromas show no signs of local invasion, nor do they show the typical morphological pat-

terns seen in sarcomas, but they grow steadily and if not removed can resemble malignant tumors in size and appearance. The finding of RFLPs in the Rb gene of these obviously benign tumors suggests that Rb alterations are not, by themselves, sufficient for malignancy. The need for additional alterations, beyond what might be occurring in the Rb gene, is entirely compatible with the two-stage model of carcinogenesis. LET-specific RFLPs may reflect intragenic alterations in a single tumor suppressor gene possibly involved in the development of radiation-induced cancers of rat skin.

Recent results with the mouse c-DNA Rb probe have not confirmed the human probe results and indicate population polymorphism in control DNA not detected by the human probe. Approximately two-thirds of the rat Rb c-DNA has been sequenced which permits the fabrication of rat-specific Rb probes. New studies with these probes are a next step in the analysys of the Rb gene in radiation-induced rat skin cancers.

Selection and growth of rat keratinocytes in Ca++ in vitro

In keratinocytes, as in other cells of epithelial origin, calcium is vital for growth but also acts to trigger the keratinocytes into terminal differentiation. For human and mouse keratinocytes, serial subculture has been accomplished in low calcium media under both serum-free and serum utilized conditions. The properties of cultured keratinocytes growing in reduced levels of calcium has been well documented for mouse, human and rat cells in short term culture. Although there are species differences in the concentration of calcium at which the cells begin to differentiate, the response itself is similar. In reduced calcium media the keratinocytes have a rounded, cobblestone appearance with wide inter-cellular spaces. The keratinocytes do not stratify but rather continue to proliferate in a monolayer.

Rat skin keratinocyte cell lines capable of serial subculture for extended periods were derived from primary cultures of neonatal rat skin keratinocytes and from rat skin carcinomas. The cell lines were isolated and maintained in serum-free, low calcium (0.09 mM) medium without the use of a feeder layer. Under such conditions the keratinocytes grew in a monolayer and did not stratify. The cultures displayed the characteristic morphology of epithelial

cells grown in low calcium medium including cobblestone appearance and wide inter-cellular spaces. This morphology remained consistent throughout the period of subculture and was independent of passage number. Positive staining of the cells utilizing a keratin-specific primary antibody confirmed their epithelial origin. A population doubling time of 36 hours was estimated from growth curves in passage 10. When switched at passage 10 to serum-free medium containing 1.8 mM calcium, the

cultures from normal tissue rapidly underwent morphological changes including a less rounded cell shape and narrowing of the inter- cellular spaces and within three weeks had stratified, formed sheets, and sloughed from the dishes. By contrast focal areas of irradiated cultures and cultures derived from skin cancers main- tained their morphology and continued to proliferate for as long as 15 weeks after being switched to high calcium. This indicates that during the subculture period the normal keratinocytes had retained the calcium-induced differentiation trigger which is characteristic of keratinocytes, while irradiated cells and cancer cells exhibited transformation to calcium independence. These results demonstrate that the subculture of rat skin keratinocytes under serum-free, low calcium conditions can be accomplished over prolonged periods without losing morphological characteristics typical of the cell type, and that growth in high calcium is a possible indicator of neoplastic transformation by irradiation.

Skin cancers in tinea capitis patients

A group of 1640 people who were exposed as children to about 3 Gy of x-rays as part of their treatment for ringworm of the scalp (tinea capitis), along with a comparable group of unirradiated controls, have been followed for skin cancer induction for nearly 35 years (48-50). The incidence of basal cell cancers in the irradiated population is currently elevated by approximately a factor of 5 in comparison to controls. An unexpectedly large percentage (about 1%) of these patients present with multiple cancers (up to 9 per patient) suggesting the possibility of a subpopulation with high susceptibility to radiation carcinogenesis. Of the 41 individuals in the x-irradiated group who developed skin cancer, 13 developed 2 or more

cancers, and 7 developed 3 or more including 3 people who developed 9, 9, and 7 cancers respectively. If the skin cancers were randomly distributed among the 1670 persons at risk, less than 1 person should have developed multiple cancers. The observation of 13 multiple cancer cases when less than 1 was expected is statistically significant and suggests the existence of a subpopulation of patients with unusual sensitivity to the carcinogenic effects of radiation.

As a pilot study to obtain information on the possible reasons for this increased sensitivity, 2 multiple cancer patients (7 and 9 cancers) were brought into the clinic and biopsy samples were obtained from an x-irradiated scalp location behind the ear and from a skin cancer. Full skin, 2.0 mm punch biopsies were obtained under aseptic conditions and fibroblasts grown from these biopsies were analyzed for chromosomal aberrations. The biopsy tissue was minced and dispersed in collagenase and incubated until a monolayer of fibroblasts was seen to be growing out and covering the culture dish. The cells were cultured in Dulbecco's modified Eagle's medium supplemented with 15% fetal bovine serum, L-glutamine (2mM), penicillin (50 units/ml), and streptomycin (50 ug/ml) in a 10% CO2 atmosphere at 30oC. The cytogenetic analysis showed aneuploidy and a high incidence of clonal and non-clonal translocations and deletions in the chromosomes. These chromosome aberrations could have been late manifestations of radiation damage occurring, in some cases, as much as 35 years after exposure to the x-ray. These findings carry no necessary implications for the majority of the original skin fibroblasts, however fibroblasts cultured from unirradiated skin show such aberrations less than 5% of the time. Observing severe chromosomal aberrations in 2 out of 2 patients is significant, although confirmation in a larger number of patients is needed.

Ionizing radiation is a potent carcinogen in animals and man. The induction of tumors in rat skin by exposure to ionizing radiation has proven useful for studies on the biological and molecular mechanisms associated with radiation carcinogenesis (89-91). We have previously found the c-*myc* oncogene to be amplified in late stage skin carcinomas induced by electron

radiation (0.8 MeV) (92,93). This amplification proved to be significantly correlated with size and age of tumors. Using serial biopsies, we determined that the c-*myc* copy number increased in individual tumors as a function of time and tumor growth (93). It appeared from our results that c-*myc* amplification in individual cells of small early tumors might allow for selective advantage and clonal outgrowth of a subpopulation of tumor cells. The rate of gene amplification has in fact been found to increase in malignant cells compared to normal cells (94) and our results could be explained if amplification of the c-*myc* gene lends a selective advantage to a tumor cell subpopulation. The relationship between c-*myc* amplification and the inducing radiation events was not clear, since we saw only low levels of gene amplification in small early lesions (93).

Amplification and over-expression of the c-*myc* oncogene has been observed in a wide variety of human and experimental animal tumors and transformed cells (95-97). Often c-*myc* activation has been associated with later stages of neoplastic progression (98-100). In contrast to the ras family, which may be activated in some cases directly by the mutational activity of the carcinogen (101,102), c-*myc* activation is often a late event, apparently not directly associated with the effects of the tumor inducing agent.

The linear energy transfer (LET) of ionizing radiation has been shown to have significant effects on many radiobiological endpoints (103-105), including rat skin carcinogenesis (106). Quantitative modeling of tumor incidence data as a function of LET and dose has shown that high and low LET radiation operate through disparate mechanisms, probably involving different number as well as types of events (106). The pattern of activating *ras* mutations in radiation-induced mouse thymomas has been shown to differ in high and low LET radiation induced tumors (107) and differential effects of high and low LET on the expression of certain genes, including c-*fos* has been observed within 3 hr after irradiation of hamster fibroblasts (108). We have examined the amplification of the c-*myc* (and selected other oncogenes) in rat skin tumors induced by high LET neon ions and compared our findings with our earlier data using low LET electrons.

The histologic profile of the panel of tumors induced by neon ions are compared with that seen using low LET. The size of these tumors ranged from 0.3 to ~ 30 cm^3. Comparison of the means and medians for tumor size, shown in, indicate a deviation from a normal distribution, with most tumors being small, with a few quite large. Growth rates of individual tumors also varied significantly, with a subpopulation (~ 10/%) growing extremely rapidly. We determined the gene copy number of c-*myc* in 70 tumors representing each histologic type, size, and growth rate. The oncogenes c-*fos*, *c-abl* and H-*ras* were analyzed in subsets of this population. Table 8 shows the frequency of gene amplification (defined as an increase in gene copy number of 3-fold or greater) as determined by Southern blot analyses in these tumors. Amplification of c-*myc* was seen in only ~ 14% of the tumors and, more importantly, was not correlated with tumor size.

For electron induced tumors we had observed a significant specificity for tissue type in c-*myc* amplification, which was completely absent in sarcomas. As seen in Table 8 such specificity was not seen for the neon ion induced tumors where the frequency of amplification in sarcomas was not different from that in carcinomas. The frequency of amplification of 3 other oncogenes in subsets of the neon-induced tumors was also quite low, with 0/13 tumors exhibiting amplified c-*fos* , 0/9 showing amplified c-*abl* and 2/17 showing amplified H-*ras*.

Based on our previous results (95), we have concluded that a low frequency (up to ~ 20%) of amplification can be detected for many genes in radiation induced tumors. The random nature of these events, with no clear connection to any biological parameters of the tumor, renders their mechanistic significance to etiology of tumors doubtful. The pattern of c-*myc* amplification shown in Table 8 suggests that the c-*myc* gene falls into this category for the neon-indu ed tumors in contrast to the situation with low LET tumors. This conclusion was supported by further statistical analysis and comparison of the role of c-*myc* amplification in the 2 tumor populations.

Tables 9 and 10 compare statistical parameters of *myc* amplification as a function of size and tumor age (time from appearance to analysis) in high and low LET-induced tumors. As

shown in Table 9, the neon-induced tumors were larger on average than the electron-induced tumors. For the high LET-induced tumors, there was no difference in size between those with and without c-*myc* amplification, whereas the low LET-induced tumors with amplified c-*myc* were on average 4 times larger than tumors with normal c-*myc*. *Linear* regression analysis of the c-*myc* gene copy number of each individual tumor showed no correlation with tumor size or growth time in neon-induced tumors, as opposed to the results using electron-induced tumors which showed significant correlation between c-*myc* and both these progression-related parameters (Table 10). No correlation was seen between the growth rate and c-*myc* gene copy number of tumors induced by either radiation.

4.1 *Discussion of Results*

It has been known for some time that mechanisms of tumorigenesis induced by ionizing radiation of low and high LET must be different. This conclusion was based partially on differences in the shape of the dose response curve. For example in rat skin, high LET radiation produces a linear response of tumor incidence, while low LET radiation induces tumors that follow a power function of dose. Models describing the quantitative contribution of LET to the tumor incidence dose response curve in rat skin have been described (89,106). Repair characteristics, as determined by split dose experiments, also differ between radiation exposures of high and low LET.

It might be assumed, based on the different patterns of energy deposition from high LET neon ions vs. low LET electrons, that differences in the mechanisms of carcinogenesis would be detectable at the molecular level. In fact, Pellicer and co- workers have demonstrated that in mouse thymomas, the pattern of *ras* gene mutational activation differ between high and low LET (107). The results of our study extend these findings to effects on the c-*myc* oncogene. However, a critical difference between the 2 studies adds a degree of complexity to interpretation of our results. While it seems likely that *ras* gene activation may be an early event in the carcinogenic process, we have previously shown that in rat skin tumors induced by electron radiation, amplification of c-*myc* appears to be a late event that is only detectable once

tumors have reached a stage well beyond initial tumor appearance (93). Furthermore, our earlier results led us to hypothesize that subpopulations of cells within the heterogeneous tumors containing amplified c-*myc*, possessed a selective advantage and with time became the dominant cell type in a rapidly growing, highly malignant tumor. This hypothesis has been supported by recent *in situ* hybridization experiments (see section 3.0).

These observations appeared to negate a direct role for the influence of the original inducing radiation in amplification of c-*myc* in late stage rat skin tumors. However, our present results contradict this conclusion, since if *myc* amplification were related to a tissue specific phenomenon only, and had no causal connection to the inducing carcinogen, then the same pattern of amplification would be observed, regardless of the energy transfer quality of the inducing radiation.

In fact, our results are consistent with the hypothesis that c-*myc* amplification in late stage carcinomas of rat skin induced by electron radiation is mechanistically linked to the radiation exposure. It is difficult, however, to conceive of a direct effect on the c-*myc* gene by the initial radiation exposure that could account for amplification of the gene in a subpopulation of tumor cells, many generations later after tumor progression has led to tumor heterogeneity. A more likely explanation is that the initial radiation exposure produces other effects in the target cell(s), that eventually lead to c-*myc* amplification in a subpopulation of the transformed cells during the later process of tumor progression and evolution. It may be speculated that cellular pathways leading to increased genomic instability that would allow a higher gene amplification frequency may be specifically activated by low LET radiation. A number of genes, including c-*jun* (108), protein kinase C, (109) and c-*fos* (110), have been shown to be induced in cells at early times (within the first 1-3 hours) after radiation exposure. Interestingly, the c-*fos* oncogene (which may play a role in the induction of genomic instability) has been shown by Woloschak and colleagues to be induced by low, but not high LET radiation (111).

A mechanism involving an early increase in genomic instability leading to enhanced pro-

bability of gene amplification does not explain the fact that only the c-*myc* gene is found to be amplified in the late stage tumors. However, this may be explained by a selection process whereby only tumor cells containing amplified c-*myc* have the necessary selective growth advantage to progress to the next level of malignancy. Studies designed to relate the early effects of ionizing radiation (as a function of LET to observations of molecular alteration in end-stage tumors are critical to achieve an understanding of the relevant mechanistic chain of events underlying radiation carcinogenesis. The rat skin model system provides an excellent tool with which to perform such studies.

Table 8. Fraction of Neon Ion Induced Tumors with Amplified c-*myc* as a Function of Size Class and Histologic Type.

	Tumor Size					
Histology	<1 cm^3		1-10 cm^3		>10 cm^3	
	High LET	Low LET	High LET	Low LET	High LET	Low LET
Carcinomas	2/8[b]	4/23	2/9	11/21	0/4	6/6
Sarcomas	0/0		0/1	2/11	0/6	1/8
Others	2/9	----	0/15	----	1/6	----

[a] Data for low LET-induced tumors is from Report # DOE/ER-60539-7.
[b] Number of tumors with c-*myc* copy number >3/total number of tumors tested.

Table 9. Comparison of Tumor Size Related to c-myc Amplification Between High and Low LET-Induced Tumors.

Radiation	LET	c-myc AMP[a]	No. Tumors
Electron	Low	-	38
	+	27	8.03 ± 2.3 p = .006
Neon	High	-	60
	+	10	6.63 ± 3.4 NS

a+ = c-*myc* gene copy number ≥ 3 compared to control.
NS = not significant.

Table 10. Correlation of c-*myc* Gene Copy Number with Tumor Size and Growth Time for High and Low LET-Induced Tumors.

Radiation		Tumor		
LET	No. Tumors	Parameter	Ra	P
High	70	Size	0.039	0.75 (NS)b
Low	65	Size	0.54	0.0001
High	69	Time	0.18	0.14 (NS)
Low	49	Time	0.40	0.004
High	67	Growth Rate	0.17	0.18 (NS)
Low	50	Growth Rate	0.16	0.27 (NS)

[a] R = Linear correlation coefficient of plot of c-*myc* copy number as determined by densitometry scanning.

[b] NS = Not significant.

FIGURE LEGENDS

Figure 1. Diagram of the events and stages in radiation carcinogenesis. Genetic alterations labeled S are envisioned to occur in association with cell division. Alterations labeled event 1 and event 2 are produced by action of low LET radiation (R_L) or high LET radiation (R_H). Two radiation-induced events are equivalent to 1 stage in the conventional multistage formalism. Clonal growth may amplify stages as depicted.

Figure 2. Examples of temporal tumor onset data. Rat skin was irradiated with electron radiation, neon ions or argon ions. The onset time of each tumor was the earliest time of visual detection. Each tumor was examined and confirmed histologically. Equation 3 was fitted to the data with n= 2.0 and w=0.

Figure 3. Tumor yield as a function of surface dose at 100 weeks after irradiation for rat skin irradiated at 28 d of age with monoenergetic electrons, neon ions or argon ions. Regression lines of the expression f(d)/D=CL + BD were fitted to the data and C & B were estimated as described in the test.

Figure 4. A plot of the percentage unrepaired (P) versus time between fractions for electron (open circles) and argon ion (closed squares) radiation. P=f(d,0)-f(d,t))/(f(D,0)-f(D,+)), where f(D,0) is the cancer yield when two equal doses of magnitude D were given with no time separating them, f(D,+) is the response when two exposures were well separated (greater than 24 hrs.) and f(D,t) is the tumor response when the two exposures were separated by time t.

Figure 5. Typical cancer incidence versus time results for single and multiple exposures of rat skin to electron radiation. Single exposure data and multiple exposure data were fitted by n=2.0 and n=6.3 respectively.

Figure 6. Gene copy number for c-*myc* as a function of time after tumor appearance. The linear correlation coefficient of the regression line shown was 0.40 ($P<0.01$). The arrow indicates a c-*myc* copy number of 3 which occurred at 14 weeks after appearance.

Figure 7. The sequence and location of the biopsies on the dorsal skin. The sequence is given by the numbers in the small rectangles. The large rectangle represents the outline of the irradiated area of dorsal skin. The midline of the long axis coincided as closely as possible to the spinal axis.

Figure 8. The labeled mitosis curve in normal unstimulated rat epidermis. The solid line is derived from the G_o model with a total length of the constant duration phase (pre S, S and G_2) of 40 hrs. Mitotic cells were accumulated for 4.0 hours by injection of vinblastine.

Data in the vicinity of the first peak have been omitted for clarity.

Figure 9. The tritium (^3H) labeling index of the basal cells of biopsy samples incubated in ^3H-thymidine at various times after the radiation doses indicated. Time zero was the time of the ^{14}C-thymidine injection. The error bars indicate the standard error of the mean count.

Figure 10. The carbon-14 labeling index of the rat basal cells at various times at the radiation doses indicated. Time zero was the time of the ^{14}C injection. The error bars indicate the standard error of the mean

count.

Figure 11. Labeled S-phase curves in rat epidermis. The proportion of S-phase cells showing ^{14}C labeling as a function of time at the various radiation doses as indicated.

Time zero was the time of the ^{14}C-thymidine injection. The error bars indicate the standard error of the mean count.

Figure 12. The proportion of ^{14C}-labeled cells entering S-phase as a function of time at the various radiation doses as indicated. Doubly labeled basal cells as a percentage of ^{14}C-labeled basal cells versus time. Time zero was the time of the ^{14}C-thymidine injection. The error bars indicate the standard error of the mean count.

Figure 13. The total number of epidermal cells per unit distance along the basement membrane on sections. The data are presented as a percentage of number at 18 hrs for each curve.

1.0 *REFERENCES*

1. Bock, F. C. Cutaneous carcinogenesis. In: Advances in Modern Toxicology, Vol. 4 (F. N. Marzulli, and H. I. Maibach, Eds.), John Wiley & Sons, New York, 1977, pp. 473-486.

2. Albert, R. E., Burns, F. J., and Shore, R. Comparison of the incidence and time patterns of radiation-induced skin cancer in humans and rats. In: *Late Biological Effects of Ionizing Radiation: Proceeding of a* Symposium, Vol. II, Vienna, 13-17 March 1978, International Atomic Energy Agency, Vienna, 1978, pp. 499-505.

3. Modan, B., Baidatz, D., and Mart, H. Radiation-induced head and neck tumors. *Lancet 1:* 277-279 (1974).

4. Armitage, P., and Doll, R. The age distribution of cancer and a multistage theory of carcinogenesis. *Brit. J. Cancer 8:* 1-12 (1954).

5. Moolgavkar S. H., Luebeck, G. Two-event model for carcinogenesis: biological, mathematical, and statistical considerations. *Risk Anal 10:* 323-341, 1990.

6. Brown, K., Buchmann, A., Balmain, A. Carcinogen-induced mutations in the mouse c-H-*ras* gene provide evidence of multiple pathways for tumor progression. *Proc. Natl. Acad. Sci. USA 87:* 538-542, 1990.

7. Iannaccone, P. M., Gardner, R. L. and Harris, H. The cellular origin of chemically induced tumors. *J. Cell Sci. 29:* 249-269, 1978.

8. National Academy of Sciences. *The Effects on Populations of Exposure to Low Levels of Ionizing Radiation,* Advisory Committee on the Biological Effects of Ionizing Radiation (BEIR), National Research Council, Washington, D.C., 1980.

9. Kellerer, A., and Rossi, H. A. Generalized formulation of dual radiation action. *Radiat. Res. 75:* 471-488 (1978).

10. Whittemore, A., and Keller, J. Quantitative theories of carcinogenesis. *SIAM Review 20:* 1-30 (1978).

11. Burns, F. J., and Albert, R. E. Dose-response for rat skin tumors induced by single and split doses of argon ions. In: *Biological and Medical Research with Accelerated Heavy Ions at the Bevalac,* University of California Press, 1981, pp. 233-236.

12. Elkind, M. M., Utsumi, H., Ben-Hur, E. Are single or multiple mechanism involved in radiation-induced mammalian cell killing? *Br. J. Cancer Suppl. 8:* 24-31, 1987.

13. Burns, F. J., Albert, R. E., Sinclair, I. P., and Bennett, P. The effect of fractionation on tumor induction and hair follicle damage in rat skin. *Radiat. Res. 53:* 235-240 (1973).

14. Vanderlaan, M., Burns, F. J., and Albert, R. E. A model describing the effects of dose and dose rate on tumor induction by radiation in rat skin. In: *Biological and Environmental Effects of Low-level Radiation, Vol. 1,* International Atomic Energy Agency, Vienna, 1976, pp. 253-263.

15. Burns, F. J., Albert, R. E., and Heimbach, R. The RBE for skin tumors and hair follicle damage in the rat following irradiation with alpha particles and electrons. *Radiat. Res. 36:* 225-241 (1968).

16. Albert, R. E., Burns, F. J., and Heimbach, R. Skin damage and tumor formation from grid and sieve patterns of electron and beta radiation in the rat. *Radiat. Res. 30:* 525-540 (1967).

17. Burns, F. J., Albert, R. E., Sinclair, I. P., and Vanderlaan, M. The effect of a 24-hour fractionation interval on the induction of rat skin tumors by electron radiation. *Radiat. Res. 62:* 478-487 (1975).

18. Burns, F. J., and Vanderlaan, M. Split dose recovery for radiation induced tumors in rat skin. *Inter. J. Radiat. Biol. 32:* 135-144 (1977).

19. Ormerod, M. G. Radiation-induced strand breaks in the DNA of mammalian cells. In: *Biology of Radiation Carcinogeneis* (J. M. Yuhas, R. W. Tennant, and J. D. Regan, Eds.), Raven Press, NY, 1976, pp. 67-92.

20. Leenhouts, H. P., and Chadwick, K. H. Radiation-induced DNA double strand breaks

and chromosome aberration. *Theor. Appl. Genet. 44:* 167-172 (1974).

21. Burns, F. J., and Sargent, E. V. The induction and repair of DNA breaks in rat epidermis irradiated with electrons. *Radiat. Res. 87:* 137-144 (1981).

22. Sawey, M. J., Hood, A. T., Burns, F. J., and Garte, S. J. Activation of K-*ras* and c-*myc* oncogenes in radiation induced rat skin tumors. *Molec. Cell Biol. 7:* 932-935 (1987).

23. Burns, F. J., and Albert, R. E. Dose-response for radiation-induced cancer in rat skin. In: *Radiation Carcinogenesis and DNA Alterations* (F. J. Burns, A. C. Upton and G. Silini, Eds.), Plenum Publishing Inc., New York, NY, 1986, pp. 51-70.

24. Land, H., Parada, L.F., Weinberg, R.A. Cellular oncogenes and multistep carcinogenesis. *Science 222:* 771-778, 1983.

25. Naoumov, N.V., Alexander, G.J., Eddleston, A.L. and Williams, R. *In situ* hybridization in formalin fixed, paraffin wax embedded liver specimens: method for detecting human and viral DNA using biotinylated probes. J. *Clin. Pathol. 41:* 793-798, 1988.

26. Burns, F.J., Albert, R.E. and Garte, S.J. Multiple stages in radiation carcinogenesis of rat skin. *Environ. Health Perspect. 81:* 67-72, 1989.

27. Wong, A.J., Bigner, S.H., Bigner, D.D. et al. Increased expression of the epidermal growth factor receptor gene in malignant gliomas is invariably associated with gene amplification. P.N.A.S. U.S.A. 84: 6899 -6903, 1987.

28. Burns, F. J., Albert, R., Altshuler, B. and Morris, E. Approach to risk assessment for genotoxic carcinogens based on data from the mouse skin initiation-promotion model. *Environ. Health Pers. 50:* 309-320, 1983.

29. Pitot, H. C., Sinica, A. E. The stages of initiation and promotion in hepatocarcinogenesis. *Biochem. Biophys. Acta. 605:* 191-215, 1980.

30. Vanderlaan, M., Strickland, P., Albert, R. E., and Burns, F. J. Age-dependence of the oncogenicity of ionizing radiation in rat skin. *Radiat. Res. 67:* 629 (1976).

31. Burns, F. J., and Vanderlaan, M. Split-dose recovery for radiation- induced tumors in rat skin. *Int. J. Radiat. Biol. 32:* 135-144 (1977).

32. Burns, F. J., and Albert, R. E. Application of a linear quadratic model with repair to rat skin carcinogenesis data. In: *Proceedings of 7th International Congress of Radiation Research* (J. J. Broerse, G. W. Barendsen, H. B. Kal, A. J. Van der Kogel, Eds.), Nijhoff Publishers, 1983, pp. C6-05.

33. Barrett, J.C., A mathematical model of the mitotic cycle and its application to the interpretation of percentage labeled mitoses data. *J. Nat. Cancer Inst. 37* : 443-450 (1966).

34. Al-Barwari, SE., Potten, CS., A cell kinetic model to explain the time of appearance of skin reaction after x-rays or ultraviolet light irradiation. *Cell Tissue Kinet 12* :281-289 (1979).

35. Boezeman, J.B., Bauer, F.W., de Grood R.M., Flow cytometric analysis of the recruitment of G_0 cells in human epidermis *in vivo* following tape stripping. *Cell Tissue Kinet (England) 20* :99-107 (1987).

36. Bohmer, R.M., Beattie, L.D., Probability of transition into cell cycle does not depend on growth factor concentration. *J Cell Physiol 136* :194-197 (1988).

37. Burns, F.J., Tannock, I.F., On the existence of a G_0-phase in the cell cycle. *Cell And Tissue Kinetics 3* :321-334 (1970).

38. Clausen, O.P., Lindmo, T., Regenerative proliferation of mouse epidermal cells following adhesive tape stripping: Micro-flow fluorometry of isolated epidermal basal cells. *Cell Tissue Kinet 9* :573-587 (1976).

39. Potten, C.S., Wichmann, H.E., Dobek, K., Birch, J., Codd, T.M., Horrocks, L., Pedrick, M., Tickle, S.P., Cell kinetic studies in the epidermis of mouse. III. The percent labelled mitosis (PLM) technique. *Cell Tissue Kinet 18* :59-70 (1985).

40. Schultze, B., Kellerer, A.M., Maurer, W., Transit times through the cycle phases of jeju-

nal crypt cells of the mouse: Analysis in terms of the mean values and the variances. *Cell Tissue Kinet 12* :347-359 (1979).

41. Skog, S., Tribukait, B., Analysis of cell flow and cell loss following x-irradiation using sequential investigation of the total number of cells in the various parts of the cell cycle. *Cell Tissue Kinet 18* :427-444 (1985).

42. Young, R.C., Devita, V.T., Perry, S., The thymidine-^{14}C and -^{3}H double-labeling technic in the study of the cell cycle of L1210 leukemia ascites tumor *in vivo Cancer Res 29* :1581-1584 (1969).

43. Voit, E.O., Anton, H.J., Estimation of cell cycle parameters from double labeling experiments. *J Theor Biol 131* :435-440 (1988).

44. Van Erp, P.E., de Mare, S., Rijzewijk, J.J., van de Kerkhof, P.C., Bauer, F.W., A sequential double immunoenzymic staining procedure to obtain cell kinetic information in normal and hyperproliferative epidermis. *Histochem J 21* :343-347 (1989).

45. Chopra, DP., Ultraviolet light carcinogenesis in hairless mice: cell kinetics during induction and progression of squamous cell carcinoma as estimated by the double-labeling technique. *J Invest Dermatol 66* :242-247 (1976).

46. Chwalinski, S., Potten, C.S., and Evans, G., Double labelling with bromodeoxyuridine and ^{3}H-thymidine of proliferative cells in small intestinal epithelium in steady state and after irradiation. *Cell Tissue Kinet 21* :317-329 (1988).

47. Burns, F.J., Theoretical aspects of growth fraction in a G_0 model. In: *The Cell Cycle In Malignancy And Immunity*

48. Burholt, D.R., Schultze, B., Maurer, W., Mode of growth of the jejunal crypt cells of the rat: An autoradiographic study using double labelling with ^{3}H- and ^{14}C-thymidine in lower and upper parts of the intestine. *Cell Tissue Kinet 9* :107-117 (1976).

49. Clausen, O.P., Thorud, E., Aarnaes, E., Evidence of rapid and slow progression of cells through G_2 phase in mouse epidermis: a comparison between phase durations measured

by different methods. *Cell Tissue Kinet 14* :227-240 (1981).

50. Ford, M.D., Martin, L., Lavin, M.F., The effect of ionizing radiation on cell cycle progression in *ataxia telangectasia. Mutat. Res. 125* :115-122 (1984).

51. Kimmel, M., Darzynkiewicz, Z., Staiano-Coico, L., Stathmokinetic analysis of human epidermal cells *in vitro. Cell Tissue Kinet. 19* :289-304 (1986).

52. Hegazy, M., Fowler, J.F., Cell population kinetics of plucked and unplucked mouse skin. *Cell Tiss. Kinet. 6* :17-0 (1973).

53. Kirkhus, B., Iversen, OH., Kristensen, A., Carcinogenic doses of methylnitrosourea induce dose response related delay in transit through S and G_2 phases in mouse epidermis: a cell kinetic study. *Carcinogenesis (United States) 8* :369-375 (1987).

54. Morris, G.M., Hamlet, R., Hopewell, J.W., The cell kinetics of the epidermis and follicular epithelium of the rat: variations with age and body site. *Cell Tissue Kinet 22* :213-222 (1989).

55. Morris, G.M., Hopewell, J.W., Changes in the cell kinetics of pig epidermis after single doses of x-rays. *Br J Radiol (England) 61* :205-211 (1988).

56. Nagasawa, H., Latt, SA., Lalande, ME., Little, JB., Effects of x-irradiation on cell-cycle progression, induction of chromosomal aberrations and cell killing in *ataxia telangietasias. Mutat. Res. 148* :71-82 (1985).

57. Pardee, A.B., Campisi, J., Croy, R.G., New directions: molecular basis of growth regulation. In: *Cancer Cells: Growth Factors And Transformation* Cold Spring Harbor laboratory, Cold Spring Harbor, NY.

58. Sauerborn, R., Balmain, A., Goerttler, K., Stohr, M., On the existence of 'arrested G_2 cells' in mouse epidermis. *Cell Tissue Kinet 11* :291-300 (1978).

59. Sargent, E.V., Burns, F.J., Radioautographic measurement of electron-induced epidermal kinetic effects in different aged rats. *J. Invest. Derm. 88* :320-323 (1987).

60. Shibui, S., Hoshino, T., Vanderlaan, M., Gray, J.W., Double labeling with iodo- and bromodeoxyuridine for cell kinetics studies. *J Histochem Cytochem 37* :1007-1011 (1989).

61. Upton, A.C. 1984. Biological aspects of radiation carcinogenesis. In: *Radiation Carcinogenesis: Epidemiology and Biological* Significance, (J.D. Boice, Jr. and J.F. Fraumeni, Jr., Eds.)pp.9-19. Raven Press, New York, NY.

62. Burns, F.J., Albert, R.E. Dose-response for radiation-induced cancer in rat skin. In: *Radiation Carcinogenesis and DNA Alterations* (F.J. Burns, A.C. Upton, and G. Silini, Eds). Plenum Publishing Inc., New York, 1986, pp.51-70.

63. Kellerer, A.M., Rossi, H.H. A generalized formulation of dual r adiation action. *Radiation Research 75:* 471-488 1978.

64. Sweigert, S.E, Rowley, R., Warters R.L., Dethlefsen, L.A. Cell cycle effect on the induction of DNA double-strand breaks by X-rays. *Radiat Res. 116:* 228-244 1988.

65. Land, H., Parada, L.F., Weinberg, R.A. Cellular oncogenes and multistep carcinogenesis. *Science 222:* 771-778 1983.

66. Roop, D.R., Krieg, T.M., Mehrel, T. et al. Transcriptional control of high molecular weight keratin gene expression in multistage mouse skin carcinogenesis. *Cancer Res. 48:* 3245-3252 1988.

67. Burns, F.J., Albert, R.E., Garte, S.J. Multiple stages in radiation carcinogenesis of rat skin. *Env. Health Pers. 81:* 67-72 1989.

68. Albert, R.E., Phillips, M.E., Bennett, P., Burns, F.J., Heimbach, R. The morphology and growth characteristics of radiation-induced epithelial skin tumors in the rat. *Cancer Research 29:* 658-668 1969.

69. Burns, F.J., Albert, R.E. Dose-response for rat skin tumors induced by single and split doses of argon ions. In: *Biological and Medical Research with Accelerated Heavy Ions at* the Bevalac. University of California Press 1981 pp.233-236.

70. Ashkenazi-Kimmel, T. 1989 Amplification of oncogenes in early-stage, radiation-induced rat skin tumors. Master's Thesis. New York University.

71. Sawey, M.J., Hood, A.T., Burns, F.J., and Garte, S.J. Activation of K- *ras* and c- *myc* oncogenes in radiation induced rat skin tumors. *Mole. Cell Biol. 7:* 932-957 1987.

72. Sawey, M.J., 1987. Activation of *myc* and ras oncogenes in radiation-induced rat skin carcinogenesis. Ph.D. Dissertation, New York University.

73. Garte, S.J., Burns, F.J., Ashkenazi-kimmel, T., Cosma, G.N., and Sawey, M.J. An experimental model for oncogene activation during tumor progression in vivo. *Anticancer Research 9:* 1439-1446 1989.

74. Kelly, K.,and Siebenlist, U. The role of c- *myc* in the proliferation of normal and neoplastic cells. *J. Clin. Immunol. 5:* 65 1985.

75. Cox, K.H., Deleo, D.V., Angerer, L.M., and Angerer, R.C. Detection of mRNA in sea urchin embryos by *in situ* hybridization using asymmetric RNA probes. *Dev. Biol. 101:* 485-501 1984.

76. Pfeifer-Ohlsson, S., Goustin, A.S., Rydnert, J., Wahlstrom, T., Bjersingn, D., and Ohlsson, R. Spatial and temporal pattern of cellular *myc* oncogene expression in developing human placenta: implications for embryonic cell proliferation. Cell 38:585 1984.

77. Hoshina, M., Boothby, M., and Boime, I. Cytological localization of chorionic gonadotropin a and placental lactogen mRNAs during development of the human placenta. *J. Cell Biol. 93:* 190-198 1982.

78. Mugrauer, G., Alt, F.W., Ekblom, P. N- *myc* Proto-oncogene expression during organogenesis in the developing mouse as revealed by *in situ* hybridization. *J. Cell Biol. 107:* 1325-1335 1988.

79. Naoumov, N.V., Alexander, G.J., Eddleston, A.L., Williams, R. *in situ* hybridization in formalin fixed, paraffin wax embedded liver specimens: method for detecting human and viral DNA using biotinylated probes. *J. Clin. Pathol. 41:* 793-798 1988.

80. Pardue, M.L. *in situ* hybridization. In: *Nucleic acid hybridization* (B.D. Hames, S.J. Higgins, Eds.). IRL Press Limited, England, 1985, pp179-202.

81. Wong, A.J., Bigner, S.H., Bigner, D.D. et al. Increased expression of the epidermal growth factor receptor gene in malignant gliomas is invariably associated with gene amplification. *Proc. Natl. Acad. Sci. USA 84:* 6899-6903 (1987).

82. Albertson, D.G., Fishpool, R., Sherrington, P. et al. Sensitive and high resolution *in situ* hybridization to human chromosomes using biotin labelled probes: assignment of the human thymocyte CD1 antigen genes to chromosome 1. *EMBO 7:* 2801-2805 1988.

83. Lee, J.H., Lee, D.H., Park, S.S., Seok, S.E. et al. Oncogene expression detected by *in situ* hybridization in human primary lung cancer. *Chest 94:* 1046-1049 1988.

84. Singer, R.H., Ward, D.C. Actin gene expression visualized in chicken muscle tissue culture by using *in situ* hybridization with a biotinylated nucleotide analog. *Proc.Natl.Acad.Sci. USA 79:* 7331-7335 1982.

85. Barbacid, M. ras genes. *Ann.Rev.Biochem. 56:* 779-827 1987.

86. Bishop, J.M. Cellular oncogenes and retroviruses. *Annu.Rev.Biochem. 52:* 301-354 1983.

87. Weinberg, R.A. The action of oncogenes in the cytoplasm and nucleus. *Science 230:* 770-776 1985.

88. Garte, S.J., Hochwalt, A. Oncogene activation in experimental carcinogenesis: The role of carcinogen and tissue specificity. *Env. Health Pers. 81:* 29-31 1989.

89. Burns, F.J. and Albert, R.E. Dose response for radiation-induced cancer in rat skin. In: *Radiation Carcinogenesis and DNA Alterations* (F.J. Burns, A.C. Upton and G. Silini, Eds.), pp. 51-70, 1986. Plenum Press, New York.

90. Burns, F.J., Albert, R.E. and Garte, S.J. Radiation-induced cancer in rat skin. *Carcinog. Compr. Surv. 11:* 293-319, 1989.

91. Burns, F.J., Albert, R.E. and Garte, S.J. Multiple stages in radiation carcinogenesis of rat skin. *Environ. Health Perspect. 81:* 67-72, 1989.

92. Sawey, M.J., Hood, A.T., Burns, F.J. and Garte, S.J. Activation of c-*myc* and K-*ras* oncogenes in primary rat skin tumors induced by ionizing radiation. Mol. *Cell Biol. 7:* 932-935, 1987.

93. Garte, S.J., Burns, F.J., Ashkenazi-Kimmel, T., Felber, M. and Sawey, M.J. Amplification of the c-myc oncogene during progression of radiation-induced rat skin tumors. *Cancer Res.* 50: 3073-3977, 1990.

94. Tlsty, T.D., Margolin, B.H. and Lum, K. Differences in the rates of gene amplification in nontumorigenic and tumorigenic cell lines as measured by Luria-Delbruck fluctuation analysis. Proc. Natl. Acad. Sci. USA 86:9441-9445, 1989.

95. Schwab, M. Oncogene amplification in neoplastic development and progression of human cancers. *Crit. Rev. Oncog. 2:* 35-51, 1990.

96. Nepveu, A., Fahrlander, P.D., Yang, J.Q. and Marcu, K.B. Amplification and altered expression of the c-*myc* oncogene in A-MuLV-transformed fibroblasts. *Nature 317:* 440-443, 1985.

97. Dalla-Favera, R., Wong-Staal, F. and Gallo, R.C. Onc gene amplification in promyelocytic leukaemia cell line HL-60 and primary leukaemic cells of the same patient. *Nature 299:* 61-63, 1982.

98. Cosma, G.N., Marchok, A.C. and Garte, S.J. Oncogene expression in cell lines derived from rat tracheal implants exposed *in vivo* to 7,12-dimethyl-benz[a]anthracene. *Mol. Carcinog. 2:* 268-273, 1989.

99. Ranzani, G.N., Pellegata, N.S., Previdere, C., Saragoni, A., Vio, A., Maltoni, M. and Amadori, D. Heterogeneous protooncogene amplification correlates with tumor progression and presence of metastases in gastric cancer patients. *Cancer Res. 50:* 7811-7814, 1990.

100. Imaseki, H., Hayashi, H., Taira, M., Ito, Y., Tabata, Y., Onoda, S., Isono, K. and Tatibana, M. Expression of c-*myc* oncogene in colorectal polyps as a biological marker for

monitoring malignant potential. *Cancer 64:* 704-709, 1989.

101. Brown, K., Quintanilla, M., Ramsden, M., Kerr, I.B., Young, S. and Balmain, A. V-*ras* genes from Harvey and BALB murine sarcoma viruses can act as initiators of two-stage mouse skin carcinogenesis. *Cell 46:* 447-456, 1986.

102. Zarbl, H., Sukumar, S., Arthur, A.V., Martin-Zanca, D. and Barbacid, M. Direct mutagenesis of Ha-ras-1 oncogenes by N-nitroso-N-methylurea during initiation of mammary carcinogenesis in rats. *Nature 315:* 382-385, 1985.

103. Afzal, S.M.J., Tenforde, T.S., Kavanau, K.S. and Curtis, S.B. Repopulation kinetics of rat rhabdomyosarcoma tumors following single and fractionated doses of low-LET and high LET radiation. *Radiat. Res. 127:* 230-233, 1991.

104. Nakamura, N., Suzuki, S., Ito, A. and Okada, S. Mutations induced by gamma-rays and fast neutrons in cultured mammalian cells. Differences in dose response and RBE with methotrexate-and 6-thioguanine-resistant systems. *Mutat. Res. 104:* 383-387, 1982.

105. Panozzo, J., Bertoncini, D., Miller, D., Libertin, C.R. and Woloschak, G.E. Modulation of expression of virus-like elements following exposure of mice to high- and low-LET radiations. *Carcinogenesis 12:* 801-804, 1991.

106. Burns, F.J., Hosselet, S., Jin, Y., Dudas, G. and Garte, S.J. Progression and multiple events in radiation carcinogenesis of rat skin. *Jap. J. Radiat. Res.* In Press.

107. Sloan, S.R., Newcomb, E.W. and Pellicer, A. Neutron radiation can activate K-*ras* via a point mutation in codon 146 and induces a different spectrum of *ras* mutations than does gamma radiation. *Mol. Cell Biol. 10:* 405-408, 1990.

108. Sherman, M.L., Datta, R., Hallahan, D.E., Weichselbaum, R.R. and Kufe, D.W. Ionizing radiation regulates expression of the c-jun protooncogene. Proc. Natl. Acad. Sci. USA 87:5663-5666, 1990.

109. Hallahan, D.E., Sukhatme, V., Sherman, M.L., Virudachalam, S., Kufe, D.W. and Weichselbaum, R.R. Protein kinase C mediates X-ray inducibility of nyuclear signal

transducers, EGR-1 and c-jun. Proc. Natl. Acad. Sci. 88:2156-2160, 1991.

110. Hollander, M.C. and Fornace, A.J. Induction of fos RNA by DNA-damaging agents. *Cancer Res. 49:* 1687-1692, 1989.

111. Woloschak, G.E. and Chang-Liu, C.M. Differential modulation of specific gene expression following high- and low-LET radiations. *Radiat. Res. 124:* 183-187, 1990.

FIGURE 1.

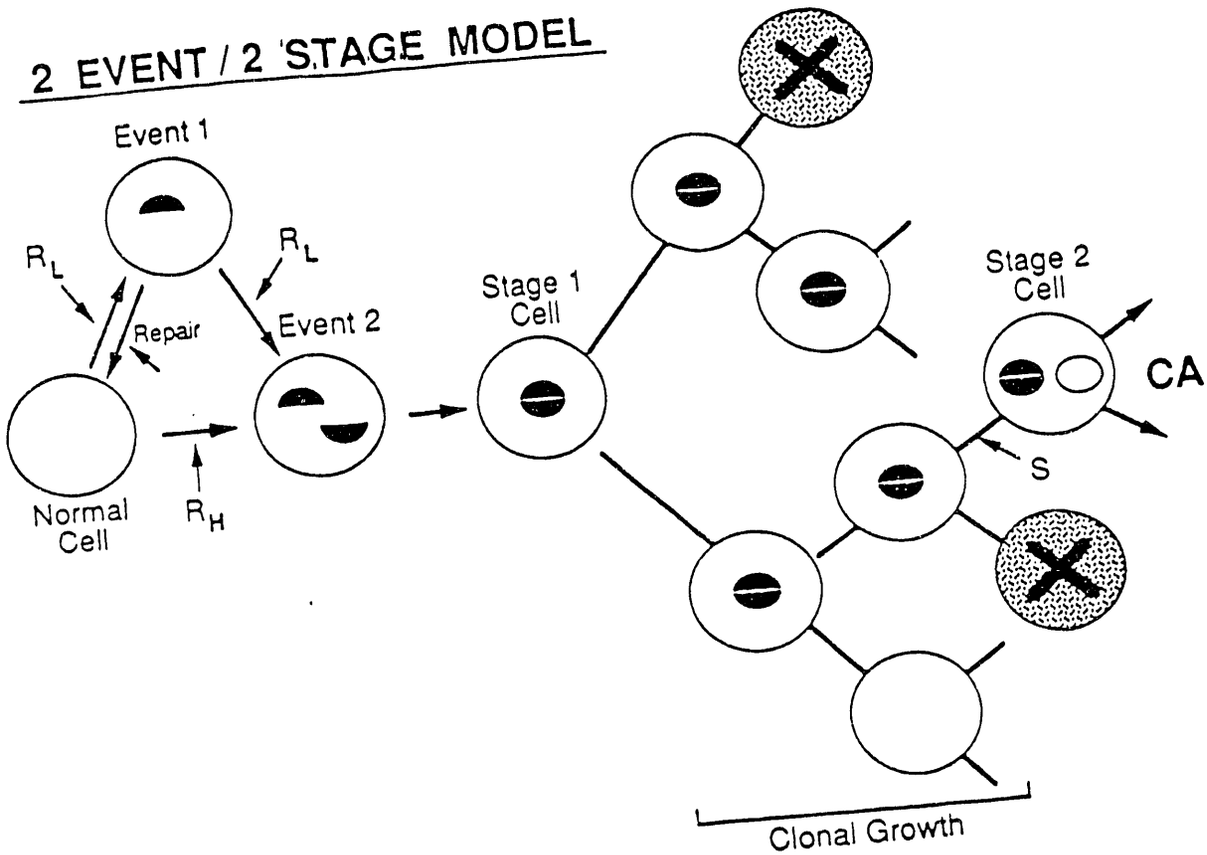

FIGURE 2.

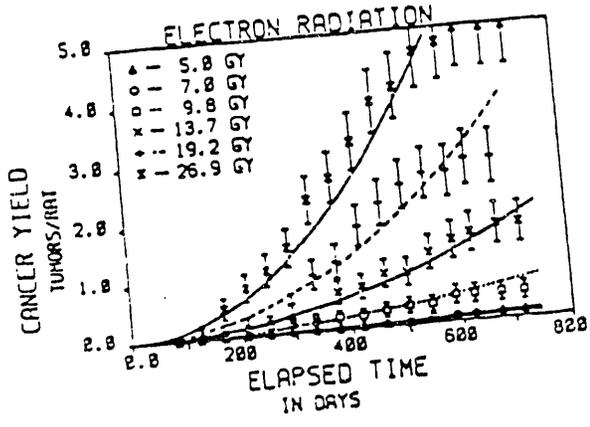

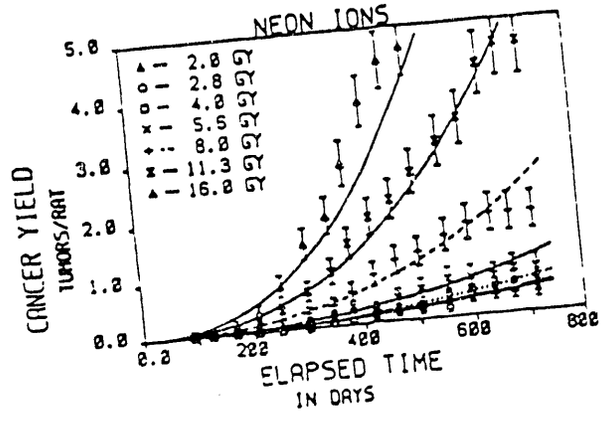

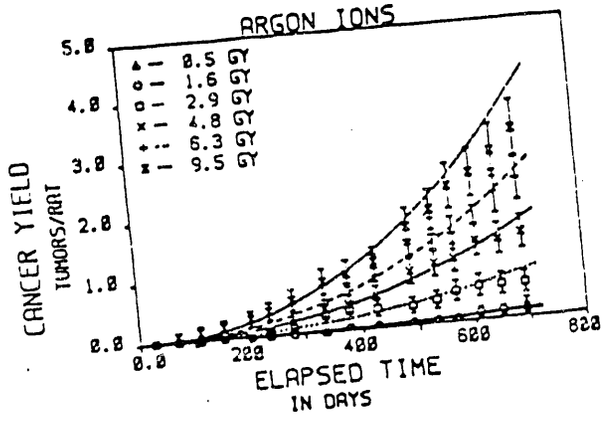

FIGURE 3.

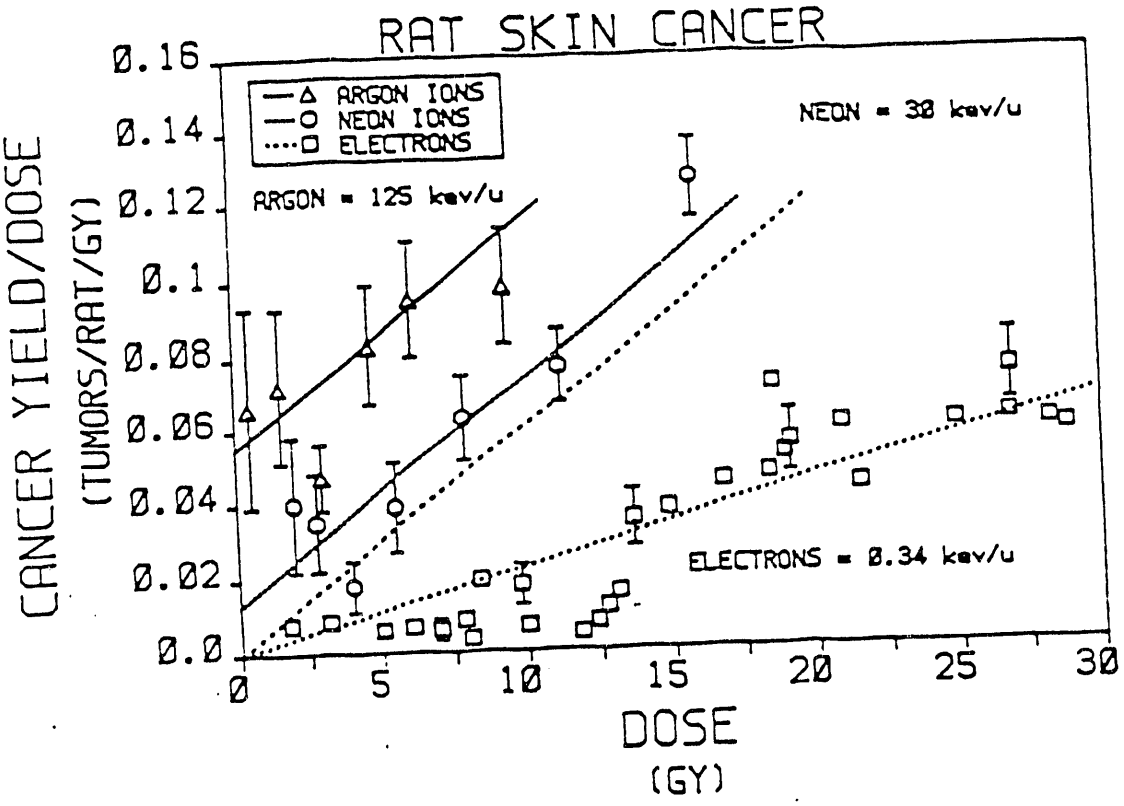

FIGURE 4.

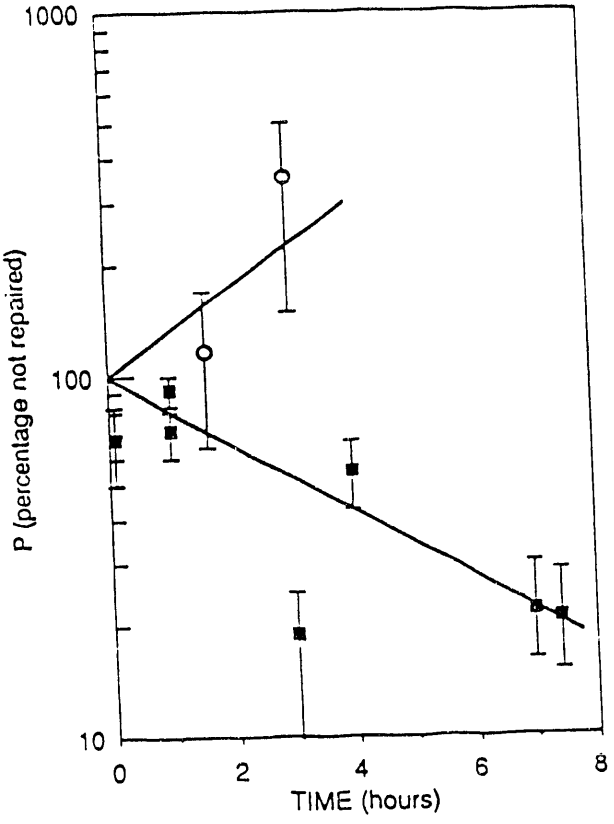

FIGURE 7.

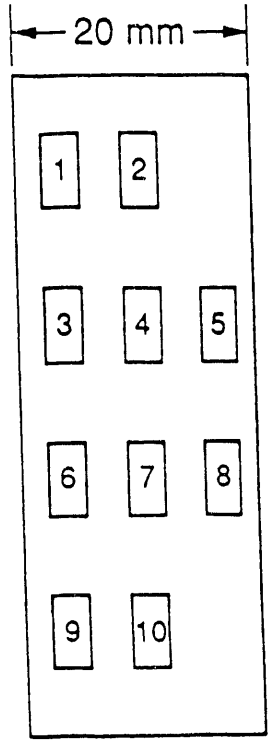

FIGURE 8.

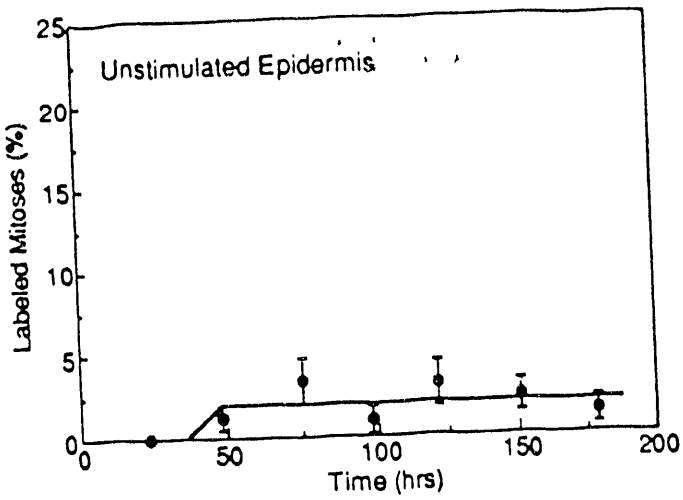

FIGURE 9.

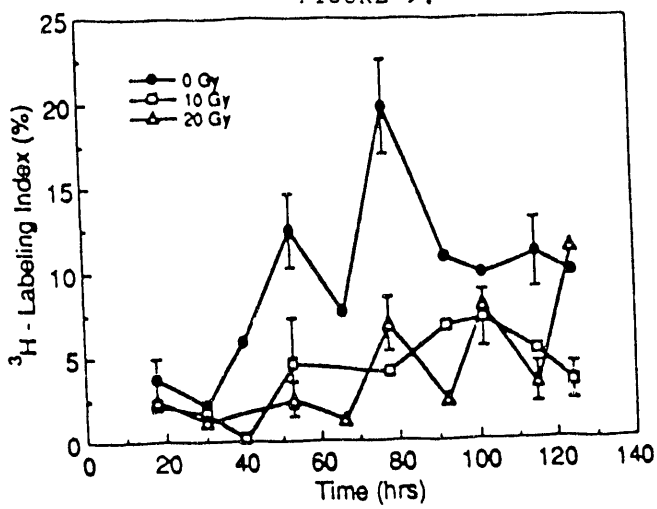

FIGURE 10.

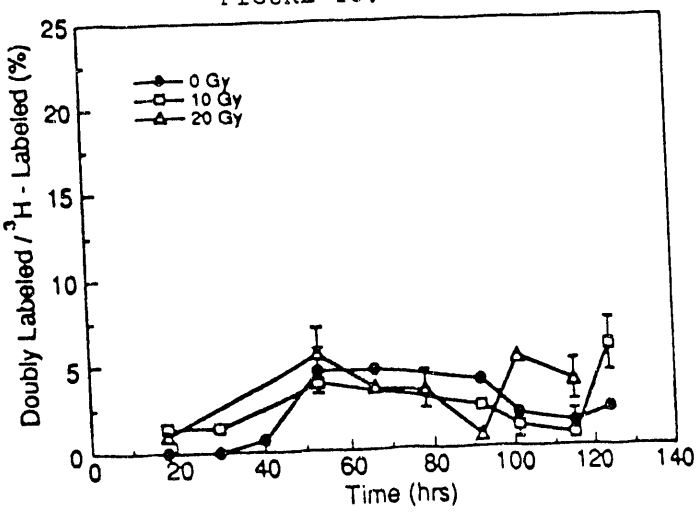

FIGURE 11.

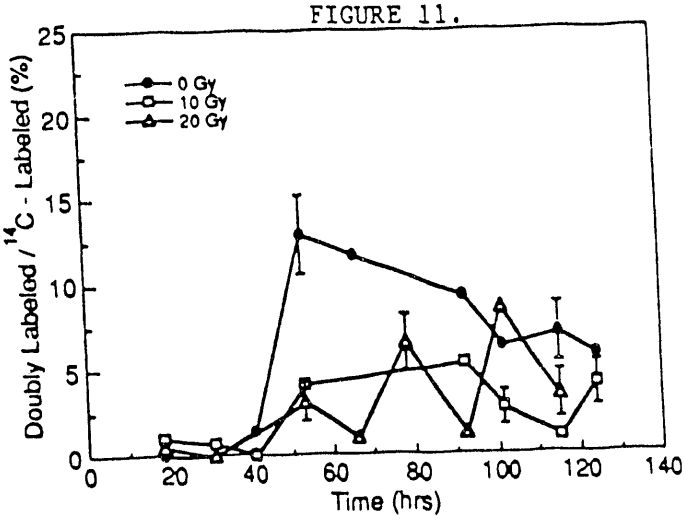

FIGURE 12.

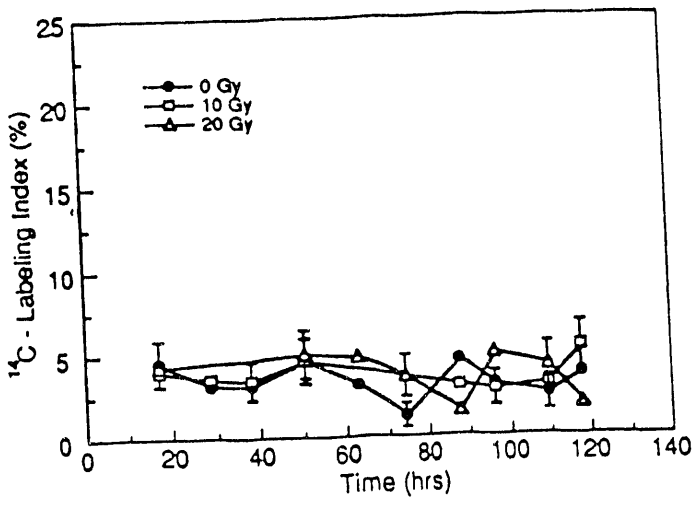

FIGURE 13.

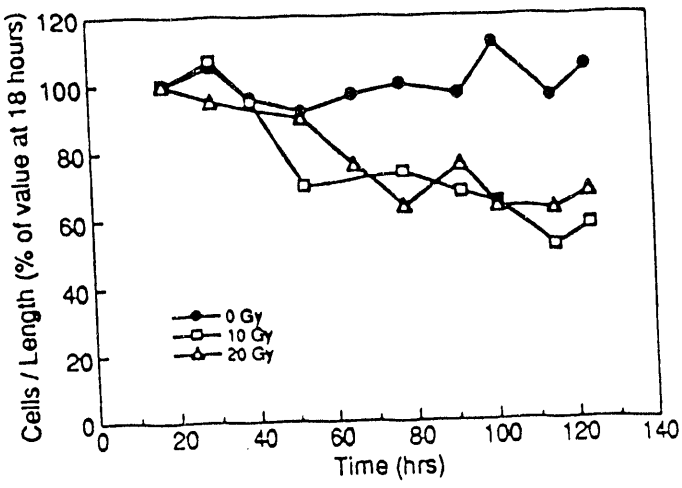

TABLE I

Distribution of Grains and Tracks in Emulsions
Average Grain and Track Counts were Determined Within the Area of a Nucleus in the First Emulsion and Within a Square 13μ on a Side in the Second Emulsion

	Cells with ^{14}C only		Cells with ^{3}H only		Background	
	Grains	Tracks	Grains	Tracks	Grains	Tracks
First Emulsion	4.3	-	90	-	1.1	-
Second Emulsion	54	6.0	12	0.8	12	0.8

TABLE II

^{3}H Labeling Index in the Vicinity of a Biopsy Wound as a Function of Time and Distance from the Wound

Time after Wound (hrs)	Distance from Wound (mm)		
	0 - 3	3 - 6	6 - 9
0	1.8	2.1	2.3
24	8.0	2.2	2.2
48	2.4	4.1	3.8
96	2.6	1.8	2.2

END

DATE
FILMED
7/13/93